

POT1 and Damage Response Malfunction Trigger Acquisition of Somatic Activating Mutations in the VEGF Pathway in Cardiac Angiosarcomas

Oriol Calvete, PhD; Pablo Garcia-Pavia, MD; Fernando Domínguez, MD; Lluc Mosteiro, PhD; Lucía Pérez-Cabornero, PhD; Diego Cantalapiedra, PhD; Esther Zorio, MD; Teresa Ramón y Cajal, MD; Maria G. Crespo-Leiro, MD; Álex Teulé, PhD; Conxi Lázaro, PhD; Manuel M. Morente, MD; Miguel Urioste, MD; Javier Benitez, PhD

Background—Mutations in the *POT1* gene explain abnormally long telomeres and multiple tumors including cardiac angiosarcomas (CAS). However, the link between long telomeres and tumorigenesis is poorly understood.

Methods and Results—Here, we have studied the somatic landscape of 3 different angiosarcoma patients with mutations in the *POT1* gene to further investigate this tumorigenesis process. In addition, the genetic landscape of 7 CAS patients without mutations in the *POT1* gene has been studied. Patients with CAS and nonfunctional *POT1* did not repress ATR (ataxia telangiectasia RAD3-related)–dependent DNA damage signaling and showed a constitutive increase of cell cycle arrest and somatic activating mutations in the VEGF (vascular endothelial growth factor)/angiogenesis pathway (*KDR* gene). The same observation was made in *POT1* mutation carriers with tumors different from CAS and also in CAS patients without mutations in the *POT1* gene but with mutations in other genes involved in DNA damage signaling.

Conclusions—Inhibition of POT1 function and damage-response malfunction activated DNA damage signaling and increased cell cycle arrest as well as interfered with apoptosis, which would permit acquisition of somatic mutations in the VEGF/angiogenesis pathway that drives tumor formation. Therapies based on the inhibition of damage signaling in asymptomatic carriers may diminish defects on cell cycle arrest and thus prevent the apoptosis deregulation that leads to the acquisition of driver mutations. (*J Am Heart Assoc.* 2019;8:e012875. DOI: 10.1161/JAHA.119.012875.)

Key Words: cardiac angiosarcoma • cell cycle arrest • damage response • POT1 • VEGF/angiogenesis pathway

The Li-Fraumeni syndrome is an autosomal dominant syndrome representing a genetic predisposition to a wide spectrum of tumors and is typically linked to mutations of the *TP53* tumor suppressor gene.¹ Li-Fraumeni-like families have a similar clinical presentation, but Li-Fraumeni-like syndrome is less frequently associated with mutations in the

TP53 gene. Recently, we studied different Li-Fraumeni-like families with multiple tumors including various cases of cardiac angiosarcoma (CAS), which is the most common and most aggressive type of primary malignant neoplasm of the heart in adults.² Patients affected with CAS are generally diagnosed at advanced stages with very poor prognosis and

From the Human Genetics Group (O.C., J.B.), Tumour Suppression Group (L.M.), Biobank Unit (M.M.M.), and Familial Cancer Clinical Unit (M.U.), Spanish National Cancer Research Center (CNIO), Madrid, Spain; Center for Biomedical Network Research on Rare Diseases (CIBERER), Madrid, Spain (O.C., J.B.); Department of Cardiology, Hospital Universitario Puerta de Hierro, Madrid, Spain (P.G.-P., F.D., M.G.C.-L.); Center for Biomedical Network Research on Cardiovascular Diseases (CIBERCV), Madrid, Spain (P.G.-P., F.D.); Facultad de Ciencias de la Salud, Universidad Francisco de Vitoria (UFV), Madrid, Spain (P.G.-P.); Spanish National Cardiovascular Research Center (CNIC), Madrid, Spain (F.D.); Medical Genetics Unit, Sistemas Genómicos, Parque Tecnológico de Valencia, Paterna, Spain (L.P.-C., D.C.); Department of Cardiology, Hospital Universitario y Politécnico La Fe, Valencia, Spain (E.Z.); Medical Oncology Service, Hospital Sant Pau, Barcelona, Spain (T.R.yC.); Department of Cardiology, Instituto de Investigación Biomédica de A Coruña (INIBIC), Complejo Hospitalario Universitario de A Coruña (CHUSIAC), A Coruña, Spain (M.G.C.-L.); Hereditary Cancer Program-Medical Oncology Service (Á.T.) and Medical Oncology Service (C.L.), Catalan Institute of Oncology, ICO-IDIBELL and CIBERONC, Barcelona, Spain.

Accompanying Tables S1 through S5 are available at <https://www.ahajournals.org/doi/suppl/10.1161/JAHA.119.012875>

Correspondence to: Oriol Calvete, PhD, Spanish National Cancer Research Center (CNIO), Melchor Fernández Almagro, 3. 28029, Madrid, Spain. E-mail: ocalvete@cnio.es or Javier Benitez, PhD, Spanish National Cancer Research Center (CNIO), Melchor Fernández Almagro, 3. 28029, Madrid, Spain. E-mail: jbenitez@cnio.es

Received April 8, 2019; accepted July 22, 2019.

© 2019 The Authors. Published on behalf of the American Heart Association, Inc., by Wiley. This is an open access article under the terms of the Creative Commons Attribution-NonCommercial License, which permits use, distribution and reproduction in any medium, provided the original work is properly cited and is not used for commercial purposes.

Clinical Perspective

What Is New?

- In this study we describe how mutations in the *POT1* gene, which explain long telomeres, correlate with cell cycle arrest increase in angiosarcoma patients.
- The same increase was observed in other cardiac angiosarcoma patients even without mutations in the *POT1* gene but in the damage response signaling.
- This malfunction would bypass the apoptosis mechanism and would trigger the acquisition of somatic activating mutations in the angiogenesis pathway.

What Are the Clinical Implications?

- Our results suggest that the use of angiogenesis inhibitors might regulate the tumor progression; however, targeting ATM/ATR (ataxia telangiectasia mutated/RAD3-related) activity would rescue the cell cycle control and would prevent the acquisition of somatic driver mutations in patients affected with angiosarcoma tumors and asymptomatic patients carrying *POT1* mutations.

short survival rates (5-year survival rate of 14%).³ The genetic landscape that determines the tumorigenic process of angiosarcomas (AS) is poorly understood and not well established.^{4,5} Previous studies by our group uncovered a deleterious missense mutation in the *POT1* gene (c.349C>T [p.Arg117Cys], pathogenic, Li-Fraumeni-like syndrome/CAS, autosomal dominant)⁶ causing AS in 4 families (3 in cardiac tissue and 1 in breast).⁶ Germline mutations in the *POT1* gene have also been related with the development of other familial cancer types.⁷⁻¹² *POT1* is a component of the so-called shelterin complex, which is involved in telomere elongation in germline and stem cells (Figure 1A).¹³ In normal conditions the shelterin complex protects telomere cap ends in somatic cells by preventing access of the telomerase to chromosome ends.¹⁴ The shelterin complex also masks single-stranded telomeres from the DNA damage response, thereby preventing the activation of ATM (ataxia telangiectasia mutated) and ATR (ataxia telangiectasia RAD3-related) to avoid cell cycle arrest through *POT1* and *TPP1* (Figure 1B).¹⁵ *TPP1* (which is also called *ACD* gene) anchors the telomere by *POT1* and *TRF1* (telomeric repeat binding factor 1) proteins. When telomeres are critically short, the shelterin complex does not prevent activation of the ATM and ATR response, which can drive the cell to senescence and apoptosis (Figure 1C).

Our previous studies demonstrated that cardiac angiosarcoma patients carrying the *POT1* p.Arg117Cys mutation showed abnormally long telomeres due to the lack of repression of telomerase, which led to increased fragility

and damage.⁶ Other described *POT1* mutations associated with risk of developing familial glioma and familial melanoma tumors also led to abnormally long and fragile telomeres.⁷ However, the link between telomere instability and tumorigenesis is not well understood. In addition, studies of the biological pathways involved in the progression of angiosarcomas are very scarce. Recently, next-generation sequencing studies uncovered somatic alterations in the VEGF/PLCG1 pathway in cardiac angiosarcoma^{16,17} and driver mutations in the PI3K/AKT/mTOR and MEK pathways in angiosarcomas other than cardiac,¹⁸⁻²¹ but these studies did not distinguish between constitutive and somatic mutations and did not clarify the genetics and underlying mechanisms.

In order to understand how telomere instability links the angiosarcoma process, in the present work we studied somatic events in different angiosarcoma patients carrying the *POT1* p.Arg117Cys mutation described in Calvete et al:⁶ 2 patients (F1 and F3) affected with CAS and 1 patient (F2) with 2 tumors, a breast AS and a papillary thyroid tumor. In addition, we studied the genetic and molecular somatic landscape that drives tumor progression in 7 patients with sporadic CAS tumors (NT1-NT3 and T1 to T4) who did not carry mutations in the *POT1* gene.

Methods

The data, methods used in the analysis, and materials used to conduct the research are available to any researcher for purposes of reproducing the results or replicating the procedure.

Ethics Statement

Institutional Review Board approval was obtained; the ethics committee of the CNIO, the Institute of Health Carlos III, and SaludMadrid (Autonomous Community of Madrid) approved this study (CS9679). Informed consent was received from participants before inclusion in the study.

Patients

Formalin-fixed paraffin-embedded (FFPE) tissue samples from 10 patients were selected. The 3 familial angiosarcoma individuals carrying the *POT1* p.Arg117Cys mutation were selected from Calvete et al.⁶ Seven FFPE tissue samples from individuals affected with sporadic CAS not carrying mutations in the *POT1* gene were also selected: 3 FFPE tissue sections contained normal (N) and tumor (T) tissue (NT1, NT2 and NT3), and the other 4 FFPE sections contained only tumor tissue (T1 to T4).

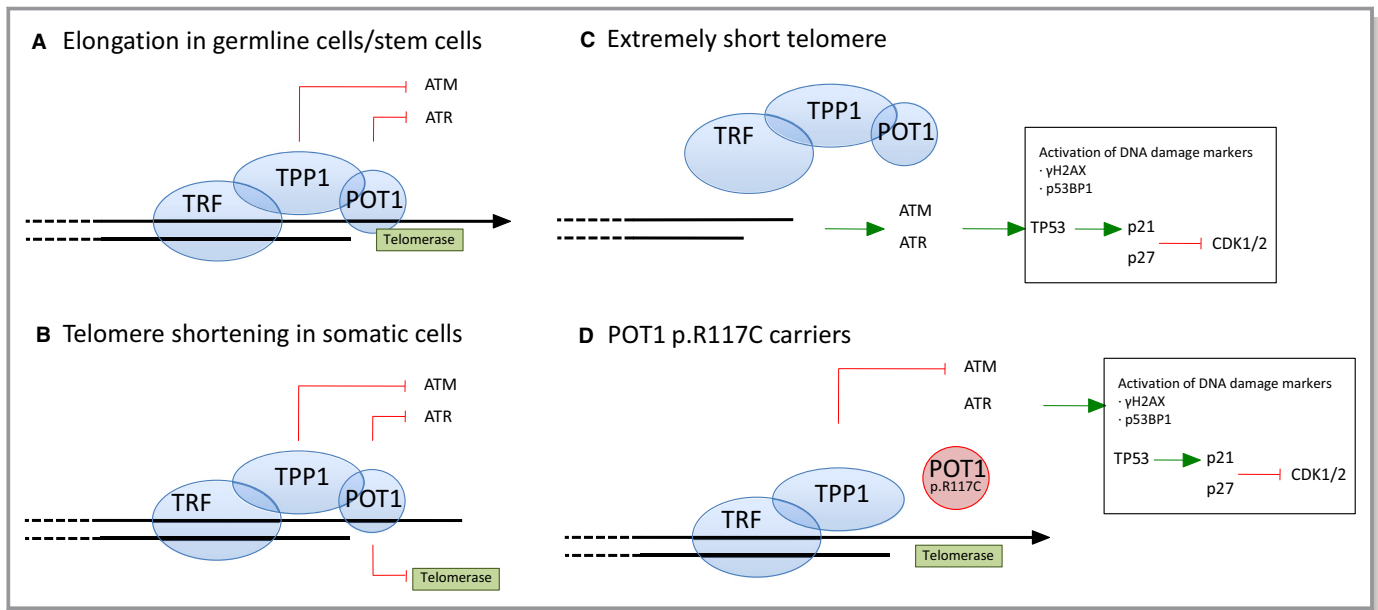


Figure 1. Telomere biology and damage signaling. **A**, Elongation in germline/stem cells. The shelterin complex mediates telomere elongation by recruiting telomerase. Shelterin also represses the DNA damage response by preventing the activation of ATM and ATR through TPP1 and POT1 proteins, respectively. TPP1 is anchored to the chromosome by POT1 and TRF (telomeric repeat binding factor 1), which is another component of the shelterin complex. **B**, Telomere shortening in somatic cells. Somatic divisions entail telomere shortening due to the inhibition of telomerase recruitment mediated by the POT1 protein. **C**, Extremely short telomere. The shelterin complex cannot bind critically short telomeres. DNA damage response ATM/ATR activates the TP53/p21 cascade to inhibit CDK1/2. DNA damage markers such as γ H2AX and TP53BP1 bind the short telomeres. DNA damage signaling mediates senescence, cell cycle arrest, and apoptosis. **D**, *POT1* p.Arg117Cys (p.R117C) mutation carriers. The *POT1* p.R117C mutation prevents POT1 from binding to TPP1 and from forming the OB-fold to bind single-strand DNA, which prevents POT1 from repressing ATR signaling. Telomere damage response is activated in *POT1* p.R117C mutation carriers.

Samples

Genomic DNA was extracted from FFPE tissue samples and from fixed tissue slides (microdissection) using the DNeasy Blood & Tissue Kit (Cat No. 69504, Qiagen, Hilden, Germany) following the manufacturer's instructions. Histology of hematoxylin and eosin-stained sections of the tissues was assessed by a pathologist (M.M.).

Immunohistochemistry

FFPE blocks were cut into 5- μ m-thick sections for immunohistochemistry (IHC) studies. The cell cycle in normal tissue was tested with anti-p21 (WAF1) from Merck (Darmstadt, Germany; Ref MABE325), anti-p27 (57/Kip1) from BD Biosciences (Franklin Lakes, NJ; Ref 610242), and anti-phosphohistone γ H2AX (Ser139) from Millipore (Burlington, MA; Ref 05-636) antibodies. Activation of the VEGF-angiogenesis pathway was assessed with 2 different antibodies against phosphorylated (activated) proteins: anti-phospho-p44/42-MAPK (ERK1/2) and anti-phospho-S6 ribosomal protein (Ser235/236) from Cell Signaling Technology (Danvers, MA; Refs 9101 and 2211, respectively). Both the absence of staining and excess nonspecific staining were considered as

negative staining. Staining was considered separately in normal (N) and tumor (T) tissues. IHC controls were performed by using normal tissue from biopsies of healthy individuals.

Whole Exome Sequencing and Bioinformatics Pipelines

Exomes from selected tissues were captured and enriched using the SureSelect Human All Exon Kit (78 Mb) (Agilent Technologies, Santa Clara, CA). Enriched samples were paired-end sequenced on an Illumina Genome Analyzer II sequencing platform using 2 lanes per sample and generating 101 base-pair long reads. FASTQ files of short reads were aligned using the BWA algorithm to the GRCh37/hg19 reference genome²²; 96.11% (ranging from 93.34% to 98.74%) of the reads aligned in the reference genomes (effectiveness). GATK-based variant calling was performed for aligned reads considering DP (Read Depth) values of >30 and Quality-by-Depth scores for a variant confidence of >1.00. A total of 92.28% (ranging from 91.70% to 92.16%) of the variants that were well aligned and annotated passed the quality and coverage filters. Strict filtering for only well-defined variants by quality controls, and those not included in repeat regions were included to prevent false positives. Tumor

variants (<10% alternative variant allele frequency) and those with low coverage (<6×) were discarded.

Only quality-filtered variants affecting coding sequences of canonical transcripts (nonsynonymous, essential splice site, frame shift or gain/loss of stops) were taken into account. Variant type annotation, population statistics, disease-specific sequence databases, and in silico predictive algorithms were according to AMCG standards and guidelines.²³ Variants with a minor allele frequency of <0.01 and <0.05 (dbSNP130, HapMap, or 1000 Genomes) were considered for stringent and relaxed filtering, respectively. Their potential damaging effect was assessed using the VEP²⁴ script software package (including Sift, Polyphen and Condel damage predictors). Stringent filtering only considered the variants annotated as pathogenic by all damage predictors. Whole-exome sequencing data have been deposited in the ArrayExpress public database under accession number E-MTAB-7999 (available at <https://www.ebi.ac.uk/fg/annotate/>).

Variants found in DNA blood samples and variants found in common between paired normal/tumor tissues were considered as constitutional. Variants found only in tumor tissue were considered somatic variants. Constitutional variants were validated in DNA from blood and normal tissue samples, and somatic variants were validated in DNA from tissue samples (tumor) by Sanger sequencing.

Pathway Enrichment Analyses

Two different software packages were used for independent assessments of the gene set analyses. Data were analyzed with Qiagen's Ingenuity Pathway Analysis (IPA, Qiagen, Redwood City, CA www.qiagen.com/ingenuity) and ConsensusPathDB (available at <http://cpdb.molgen.mpg.de/>).²⁵ Overrepresentation analysis of the gene set list was performed with a minimum overlap of 4 genes with the pathway database set size and a *P*-value cutoff of 0.001. Induced network module analysis without intermediate nodes and considering high-confidence binary protein and genetic/gene regulatory interactions were also evaluated.

Trusight Tumor 170 Panel and IBM Watson Study

Resequencing of tumor DNA from FFPE tissue samples was performed with TruSight Tumor 170 from Illumina (San Diego, CA), a novel sequencing platform that predicts the most probable variant causing the pathology and provides suggestions for translating the data to the clinic. The sequencing of the hybrid capture was run on the HiSeq 2500 System. The captured gene content in the TruSight Tumor 170 Assay, data sheet, and specifications are available at <https://www.illumina.com>. Low variant quality of <20 and low depth (<100 for variant calls and <250 for reference call filters) were considered. Variants were

supported with >7 reads and filtered by frequency (minor allele frequency <0.05). The copy number variation call was calculated for the fold-change results for each gene. Variants were classified and analyzed later by the IBM Watson for Genomics platform, which searches electronic medical databases to find information that may be relevant to a particular genomic sequence (available at <https://www.ibm.com/watson/>).

Results

Angiosarcoma Patients Carrying the *POT1* p.Arg117Cys Mutation

Constitutional Effect in Normal Tissue of *POT1* p.Arg117Cys Mutation Carriers

In normal conditions the POT1 protein represses downstream activation of the DNA damage response at telomeres in somatic cells (Figure 1B).¹⁵ The POT1 p.Arg117Cys protein shows a reduced capacity to bind telomeres and TPP1⁶ and may affect the regulation of the damage response. Damage response activation leads to cell cycle arrest, replicative senescence, and apoptosis (Figure 1C). In order to decipher the putative effect of POT1 malfunction, patient tissues were stained with anti-P-γH2AX (DNA damage marker) and anti-p21 and anti-p27 antibodies (inhibitors of CDK1/2 to arrest the cell cycle). IHC studies were carried out in normal (N) tissues of patients from the families carrying the constitutional *POT1* p.Arg117Cys mutation studied in Calvete et al⁶: 2 patients (F1 and F3) affected with CAS and 1 patient (F2) with 1 breast AS and 1 papillary thyroid tumor.

Increased IHC staining with anti-p21, -p27, and -P-γH2AX antibodies was observed in N tissues of all studied patients in comparison with the corresponding N tissues from healthy non-mutation carriers (Table 1 and Figure 2A). Therefore, the reduced binding to telomeres and to TPP1 by the POT1 p.Arg117Cys protein correlates with activation of damage response signaling mediated by p21 and p27 (Figure 1D).

Somatic Events in *POT1* p.Arg117Cys Mutation Carriers

To evaluate possible somatic events in affected individuals carrying the *POT1* p.Arg117Cys mutation that might lead to the formation of AS, the exomes of normal (N) and tumor (T) tissues of the F1 and F2 individuals were sequenced. Variants found in T tissue but not in N tissue were considered to be somatic (Table S1). In patient F1 (CAS), 46 filtered somatic variants were found in T but not in N cardiac tissue (Table 2) including an in-frame deletion in the *KDR* gene (p.Asn704del), which encodes VEGF receptor 2 (VEGFR2), which belongs to the VEGF-angiogenesis signaling pathway (Figure 3A and 3B).

Regarding the F2 individual, only 13 filtered somatic variants were found in the T tissue of the breast AS

Table 1. Total Cases and Number of Variants Found in the Whole Exome Sequencing

	Individual	Pathology	Tissue	Variant Calling	Filtered Variants	Somatic Variants*	Constitutional Variants†
<i>POT1</i> p.Arg117Cys carriers	F1	CAS	T		1095	46	NA [‡]
			N				
	F2	Papillary thyroid	T	100 506	1294	5	NA [‡]
			N	100 371	1281		
	Breast AS	T	93 496	1276	13	NA [‡]	
Without mutations in the <i>POT1</i> gene	NT1	Sporadic CAS	T	102 560	1266	62	1032
			N	111 686	1333		
	NT2	Sporadic CAS	T	100 120	1231	36	1101
			N	141 248	1239		
	NT3	Sporadic CAS	T	97 233	704	37	1180
			N	113 358	762		
	Individual	Pathology	Tissue	Variant Calling	Filtered Variants	Stringent Filtering	
Only T tissue available [‡]	T1	Sporadic CAS	T	93 374	1181	315	
	T2	Sporadic CAS	T	95 492	1274	403	
	T3	Sporadic CAS	T	104 545	1328	443	
	T4	Sporadic CAS	T	93 859	1233	361	

CAS indicates cardiac angiosarcoma; N, normal tissue; NA[‡], not applicable (*POT1* p.Arg117Cys carriers from Calvete et al [2015]); T, tumor tissue.

*Variants found in tumor tissue that were not found in normal tissue.

†Variants found in normal tissue that were not found in tumor tissue.

‡Individuals with only T tissue sequenced.

(Table S1). Two of them were variants annotated in the genes *PLCG1* (p.Leu752Val) and *PIK3CA* (p.Arg88Gln) belonging to the VEGF-angiogenesis pathway and previously described to be involved in different angiosarcomas and primary breast cancer.²⁶ Another 5 somatic variants were found in the papillary thyroid T tissue from the same individual (Table S1). Three of these belonged to the VEGF-angiogenesis pathway (*PIK3R6* [p.Arg59Lys], *RASSF1* [p.Arg227His], and *BRAF* [p.Val600Glu]). Overall, 32/52 (62%) of the somatic missenses were C:G>T:A changes (Table S1). Genes with mutations are shown in the angiogenesis pathway depicted in Figure 3.

Finally, only cardiac tumor tissue from patient F3 (CAS) was sequenced (Table 2). A total of 297 filtered variants were found in the tumor tissue of this patient (Table S2), including another mutation in the *KDR* gene (p.Thr771Arg). Overall, 60% of the somatic variants found in patient F3 were annotated as C:G>T:A changes (Table S2).

Thus, somatic mutations in the VEGF signaling pathway were found in the tumor tissues of all affected individuals carrying the *POT1* p.Arg117Cys germline mutation. Interestingly, both studied CAS patients had mutations in *KDR*, which activates VEGF signaling to regulate angiogenesis by the MAPK/ERK and AKT/PI3K pathways (Figure 3A and 3B). MAPK/ERK regulates proliferation activity, while AKT/PI3K promotes protein synthesis. Interestingly, both molecular activities regulate the cell cycle by inhibiting senescence

promotion (Figure 3C). In order to test the putative effects of the mutations found in the VEGF angiogenesis pathway, we studied the MAPK/ERK and AKT/PI3K molecular pathways by IHC with antibodies against the activated (phosphorylated) forms of ERK and S6, respectively (Figure 3A and 3B). All angiosarcomas (CAS and the breast AS tumors) did not stain with anti-P-ERK but were positively stained (>70%) with the anti-P-S6 antibody. However, papillary thyroid tumor tissue stained with both antibodies (Table 1 and Figure 2B).

In summary, somatic activating mutations of the VEGF-angiogenesis pathway were found in all studied tumor tissues of *POT1*-mutated patients independently of the tumor type (cardiac, breast, and thyroid). Somatic mutations in the *KDR* gene were found in both CAS patients (F1 and F3). In addition, positive P-S6 staining was observed in all angiosarcomas with somatic mutations in the *KDR* (CAS) and *PI3K* (breast AS) genes (AKT/PI3K pathway). The papillary tumor (F2), which had a mutation in the MAPK/ERK signaling pathway (*BRAF* gene), was stained with both anti-P-ERK and anti-PS6 antibodies (Figures 2B and 3).

Sporadic Cardiac Angiosarcoma Patients Without Mutations in the *POT1* Gene

To assess the whole genetic landscape of CAS tumors, another 7 patients with sporadic CAS tumors who were not

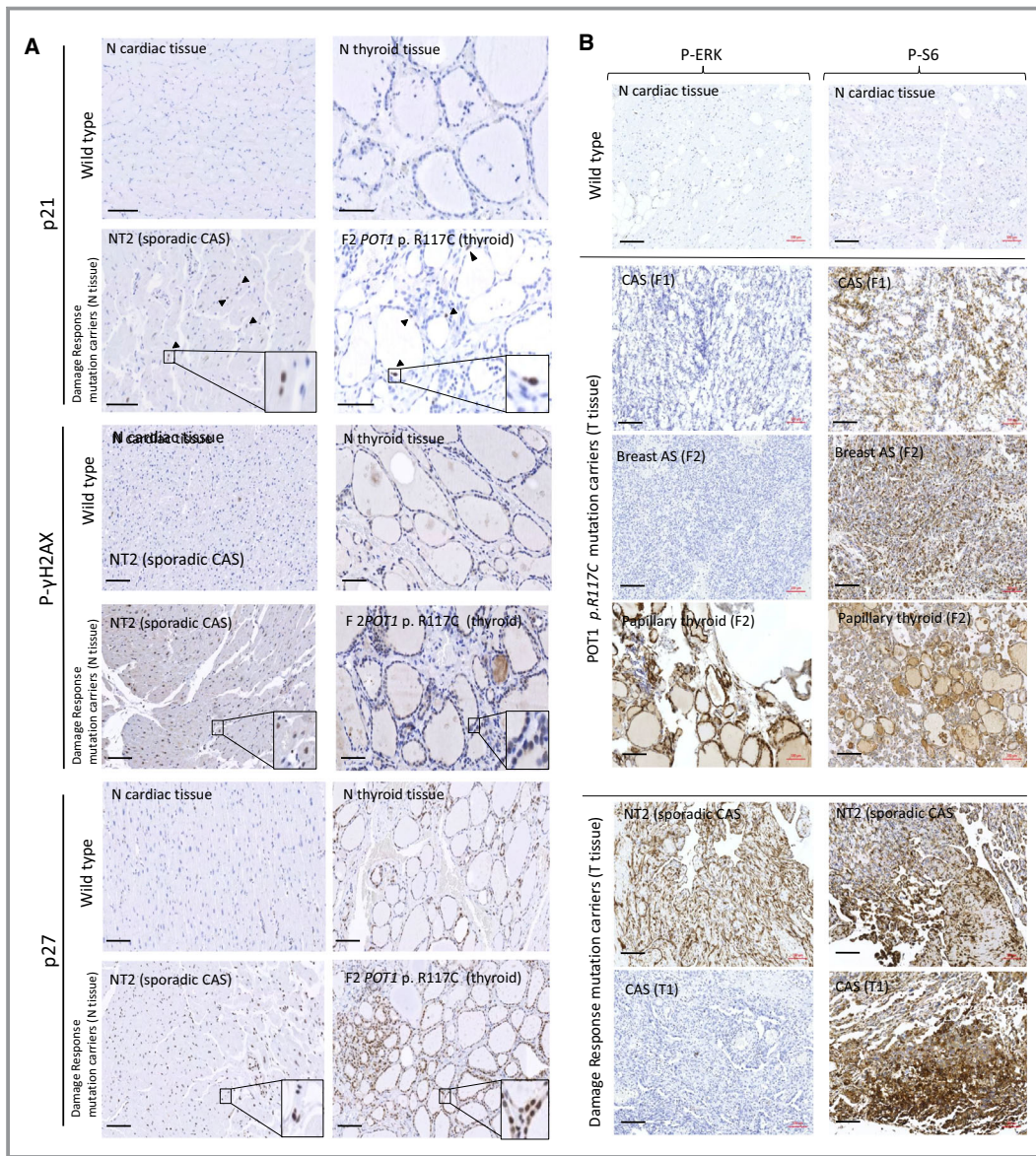


Figure 2. Immunohistochemical staining. **A**, Tissue stress was tested in normal tissue of carriers of the *POT1* p.Arg117Cys (p.R117C) mutation and carriers of mutations in the damage response–signaling pathway (sporadic CAS) in comparison with the corresponding normal tissue without mutations (wild type). Above: Wild-type cardiac and thyroid tissues from healthy controls without mutations. Below: normal tissue of individual NT2 (sporadic CAS) individual with constitutional mutations in the *ATR*, *ATM* and *TP53BP* genes) and normal tissue of individual F2 (papillary thyroid tumor with *POT1* p.R117C mutation) as representative examples (see Table 2 for all studied individuals). Increased cell cycle arrest was observed in the normal tissue of both patients. Black arrowheads show some of the stained nuclei. Detailed fields (10 \times) are also shown. Scale bar (in black): 100 μ m. **B**, IHC staining with anti-P-ERK and anti-P-S6 antibodies in tumor tissues. Tumor tissues from carriers (F1 and F2) and noncarriers (T1 and NT2) of the *POT1* p.R117C mutation compared with a normal tissue section (negative staining) are shown as examples (see Table 2 for all studied individuals). Three tumors from the 2 patients (F1 and F2) carrying the *POT1* p.R117C mutation are shown: both angiosarcomas (CAS tumor tissue from F1 and breast AS from patient F2) only showed immunoreactivity with anti-P-S6 antibody, while the papillary thyroid tumor (patient F2) also showed immunoreactivity with anti-P-ERK antibody. Two staining patterns were observed in sporadic CAS patients without mutations in the *POT1* gene: tissue from patient T1 only showed immunoreactivity with anti-P-S6, whereas tissue from patient NT2 (sporadic CAS) was stained with both anti-P-S6 and anti-P-ERK antibodies. Scale bar (in black): 100 μ m. AS indicates angiosarcoma; CAS, cardiac angiosarcoma; N, normal tissue; T, tumor tissue.

carrying mutations in the *POT1* gene were studied. Normal (N) and tumor (T) cardiac tissues were available from 3 sporadic CAS individuals (NT1, NT2, and NT3), whereas only tumor tissue was available from the other 4 CAS individuals (T1 to T4). We found 1032, 1101, and 1180 constitutional variants in cardiac tissue for the NT1, NT2, and NT3 CAS individuals, respectively; 62, 36, and 37 somatic variants were found for individuals NT1, NT2, and NT3, respectively (Table 2).

Regarding the 4 tumor samples of which only T tissue was available, no distinction could be made between constitutional and somatic variants. We found 1181, 1274, 1328, and 1233 variants in the T tissue of patients T1, T2, T3, and T4, respectively (Table 2).

To further delineate the genetic landscape of sporadic CAS tumors, the genes encompassing filtered variants were grouped into 2 different pathway enrichment analyses. The first set included genes with constitutional (found in both N and T tissues from cases NT1, NT2, and NT3) and all genes with variants from the other 4 CAS individuals with only the tumor tissue sequenced (constitutional or somatic) (2501 unique genes in total); the second set included the genes with somatic variants (only present in T tissue) from cases with N and T tissue (NT1, NT2, and NT3) and again all genes with variants from the other 4 CAS individuals with only the sequenced T tissue cases (T1 to T4) (1522 unique genes in total).

Constitutional Events in Normal Tissue in Sporadic CAS

This study revealed that the most represented pathway and the pathway with the major number of genes were the “Sustainability of p53 pathway” (genes *ATM*, *TP53*, and *RFWD2*) (*P* value 0.003) and the “Repair modulation pathway” (genes *ATR*, *ATM*, *TP53*, *RFWD2*, *SIRT7*, *BRCA2*, *CDK8*, *UBE2D1*, *WRN*, *PMS2*, *BRIP1*, *TP53BP2*, and *APC2*) (*P* value 0.0022), respectively (Table S3). Mutations in genes from these pathways were found in all 7 sporadic CAS individuals

(Figure 4). These genes belong to the damage response signaling pathway and may deregulate the cell cycle in the same manner as previously observed for the *POT1* mutation carriers. Thus, N cardiac tissue from the sporadic CAS individuals (NT series) was also stained with anti- γ H2AX, anti-p21, and anti-p27 antibodies. Positive staining was also observed in N tissue of sporadic CAS individuals (Table 1), which correlated with cell cycle deregulation as observed in familial angiosarcomas (*POT1* p.Arg117Cys mutation carriers). Therefore, the familial angiosarcomas (*POT1* p.Arg117Cys carriers) and sporadic CAS patients behaved in a similar way regarding cell cycle arrest regulation.

Somatic Events in Tumor Tissue in Sporadic CAS

A second pathway enrichment analysis was performed with the gene set including the somatic variants found in T tissues of sporadic CAS individuals (see above). This enrichment analysis revealed that the most represented pathway was the “gf-hypoxia and angiogenesis” pathway (Biocarta: 16.7%) (*P* value 0.00557). The pathway with the major number of affected genes was the “Signaling by VEGF” pathway (Reactome, 24 genes) (*P* value 0.00101) (Table S3). Both enrichment analyses corresponded with the VEGF-angiogenesis pathway. Genes with mutations are shown in the angiogenesis pathway of Figure 3. Mutations in genes from these pathways were found in all 7 sporadic CAS individuals (Figure 4). Activation of the MAPK/ERK and AKT-PI3K pathways was studied by IHC with anti-P-ERK and anti-P-S6 antibodies, respectively.

Tumors of all studied sporadic CAS individuals (NT and T series) stained positive with anti-PS6 antibodies, which demonstrates that somatic mutations were activating the VEGF-angiogenesis pathway (Table 1). Especially intense staining was also observed in the endothelial lining of blood vessels. However, not all tissues from individuals affected with sporadic CAS stained with anti-PERK antibody. Tissue of

Table 2. Immunohistochemistry Staining Results for the Studied Cases

Mutation	Sample	Pathology	Tissue	N Tissue			Mutations in VEGF-Angiogenesis Pathway	T Tissue	
				γ H2AX	p21	p27		P-ERK	P-S6*
<i>POT1</i>	F1	CAS	Cardiac (N+T)	+	+	+	<i>KDR</i>	–	+
p.Arg117Cys	F2	Breast AS	Breast T	NA	NA	NA	<i>PI3K</i>	–	+
			Thyroid (N +T)	+	+	+	<i>BRAF</i>	+	+
DR genes	NT2	CAS	Cardiac (N+T)	+	+	+	VEGF2/RAS-MAPK	+	+
	T1	CAS	Cardiac (T)	NA	NA	NA	Akt-PI3K	–	+
	T3	CAS	Cardiac (T)	NA	NA	NA	RAS-MAPK/Akt-PI3K	+	+
	T4	CAS	Cardiac (T)	NA	NA	NA	VEGFA/Akt-PI3K	+	+

+ indicates overexpression; –, no expression; CAS, cardiac angiosarcoma; DR, damage response; N, normal; NA, tissue not available; T, tumor.

*Positive staining in lining epithelium and tissue.

individual T1, who only had mutations in the AKT-PI3K signaling pathway (Table 1), did not stain with anti-P-ERK. The tumors with mutations in the 2 molecular signaling pathways (NT1, NT2, and T4) also stained positive with the 2 antibodies (anti-P-ERK and anti-P-S6) (Table 1). Interestingly, the individual with mutations only in the MAPK/ERK signaling pathway (T3) also stained positive with both antibodies (Table 1). Stained tissues from patients T1 and NT2 are shown in Figure 2B as representative examples.

In summary, all studied individuals with CAS (either familial or sporadic) had mutations (either constitutional or somatic) in normal tissue affecting damage response signaling (Figure 4). IHC with anti-p21 and anti-p27 antibodies confirmed cell cycle arrest deregulation in N tissue that leads to constitutional cell cycle arrest and cessation of cell division (Figure 2A and Table 1). In addition, somatic activating mutations in the VEGF-angiogenesis pathway were found in tumor tissue of familial and sporadic angiosarcomas, independently of the presence of *POT1* mutations (Figures 2B and 4; Table 1).

Sequencing Replication With the Truseq170 Panel and IBM Watson for Genomics Platform

A sequencing replication was performed for 2 previously sequenced CAS patients without mutations in the *POT1* gene. The Truseq170 panel was run for tumor tissue of the T1 and T4 individuals and analyzed with the IBM Watson for Genomics platform (version 33.148), which is a novel sequencing platform that predicts the most probable variant causing the pathology and provides suggestions for translating the data to the clinic. The Watson for Genomics pipeline revealed 15 variants of unknown significance, 2 alterations without proposed therapies, and only 1 actionable alteration for patient T1 (Table S4). Three variants of unknown significance, 3 alterations with no proposed therapies, and another 3 actionable alterations were described for patient T4 (Table S5). Interestingly, a not previously detected copy number gain was found for the *KIT* gene in the tumor tissue of patient T1. The gained region is involved in tumor cell proliferation, angiogenesis, and metastatic disease. Only 1 actionable pathway was found in common for both CAS patients. The variants found in the *TP53* gene were highlighted as actionable alterations, as previously found in the WES study (*TP53* p.Arg175His and *TP53* p.Val143Met for patients T1 and T4, respectively). No Food and Drug Administration–approved therapies for angiosarcoma were recommended for these 2 patients, but 3 therapies with clinical trials were observed in common for both patients: AZD1775 (NCT numbers NCT02576444 and NCT018227384), Transferrin Receptor-Targeted Liposomal p53 (NCT02354547), and Modified Vaccinia Virus Ankara Vaccine (NCT02432963). The 3

therapies for the alterations common to the 2 CAS patients target TP53 to restore cell cycle regulation.

Discussion

Telomere Instability in *POT1* Mutation Carriers Increases Cell Cycle Arrest in Constitutional Tissue and Increases Acquisition of Somatic Mutations in the Angiogenesis Pathway

The single-strand DNA response in telomeres is inactivated by the shelterin complex (Figure 1A and 1B).¹⁵ We previously observed that the *POT1* p.Arg117Cys mutation prevented the POT1 protein from binding to TPP1 and forming the OB-fold to bind single-strand DNA, which led to abnormally long telomeres.⁶ Here, we observed that abnormal telomere length found in our patients correlates with a genomic instability scenario that, in consequence, activates DNA damage-signaling (γ H2AX-positive staining). Individuals carrying the *POT1* p.Arg117Cys mutation overexpressed the p21 and p27 proteins in constitutional tissue (Table 1), which correlates with prevention of the repression of ATR signaling and leads to cell cycle arrest (Figure 1D). This increased senescence in nontumor tissue would result in reduced cell cycling and cessation of cell division. A similar mechanism was proposed to explain how short telomeres can lead to vascular senescence and diminished proliferative capacity that involved exhaustion of cell pools in mice.^{27,28} In addition, tumor tissue of *POT1* p.Arg117Cys mutation carriers was studied in order to evaluate the involvement of constitutional cell cycle arrest in tumor progression. On average, 61% of the somatic variants found in these patients were C:G>T:A changes (Tables S1 and S2). At this time we cannot rule out a correlation between this observed bias and a specific mutation signature in these tumors. Megquier et al²⁹ have established an association with somatic deamination of cytosine to thymine in a large series of angiosarcomas (different from cardiac), which is in agreement with our observation. Somatic mutations in the VEGF-angiogenesis pathway were found in tumor tissue of all individuals (Figure 4). Interestingly, the F1 and F3 individuals (CAS) also had a somatic mutation in the *KDR* gene, which is involved in VEGF/PLCG1 activation and was described altered in 2 recently studied sporadic CAS cases.^{16,17} In the F2 patient the recurrent somatic mutations *PIK3CA* p.Arg88Gln and *BRAF* p.Val600Glu were found in the breast AS and the papillary thyroid tumor, respectively. Twenty-five percent of all breast cancers have somatic mutations in the *PIK3CA* gene. Specifically, the *PIK3CA* p.Arg88Gln mutation was described in a primary breast cancer.²⁶ The somatic mutation *BRAF* p.Val600Glu is the most common genetic change in papillary thyroid cancers (35.8%).³⁰ In addition, the

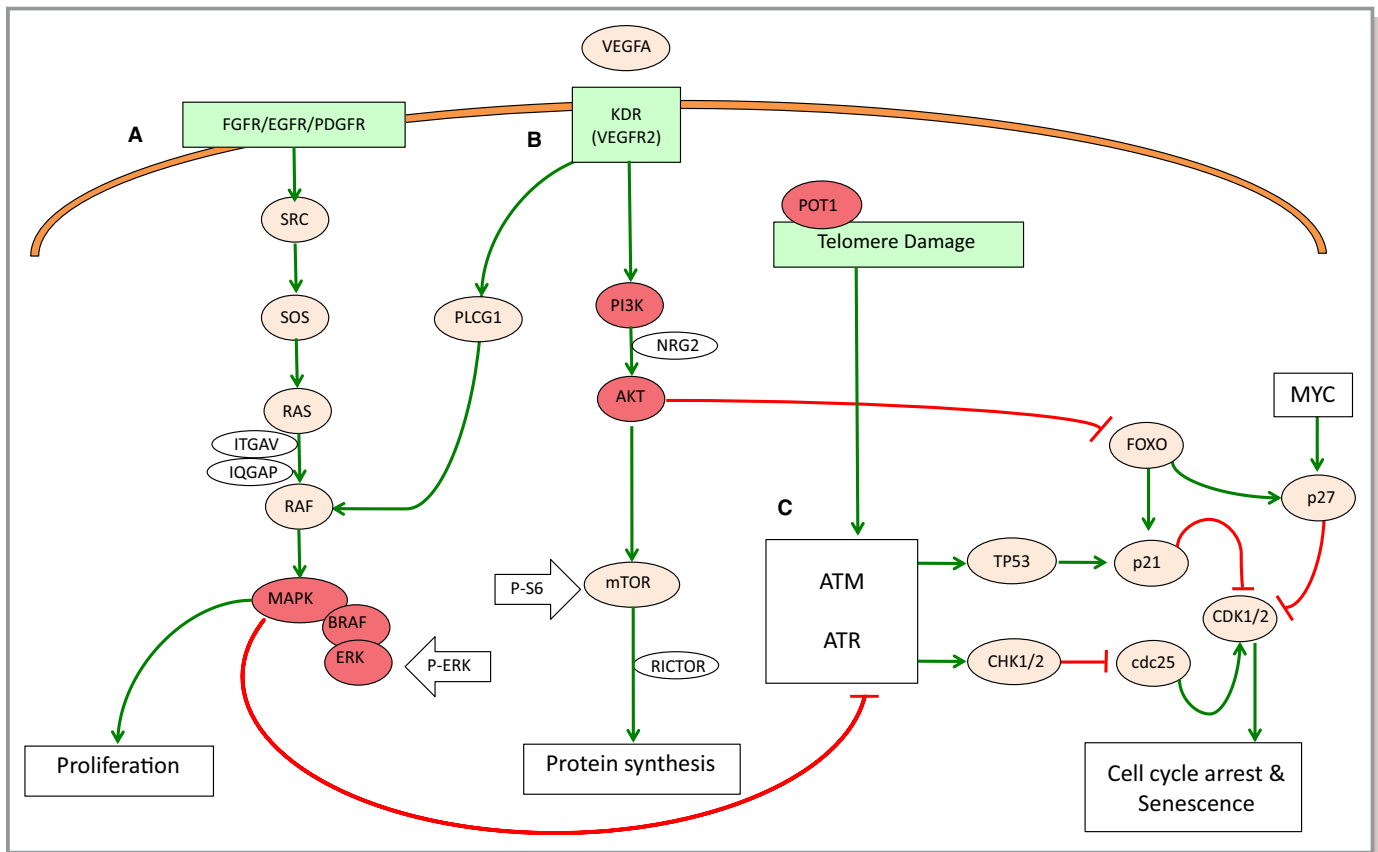


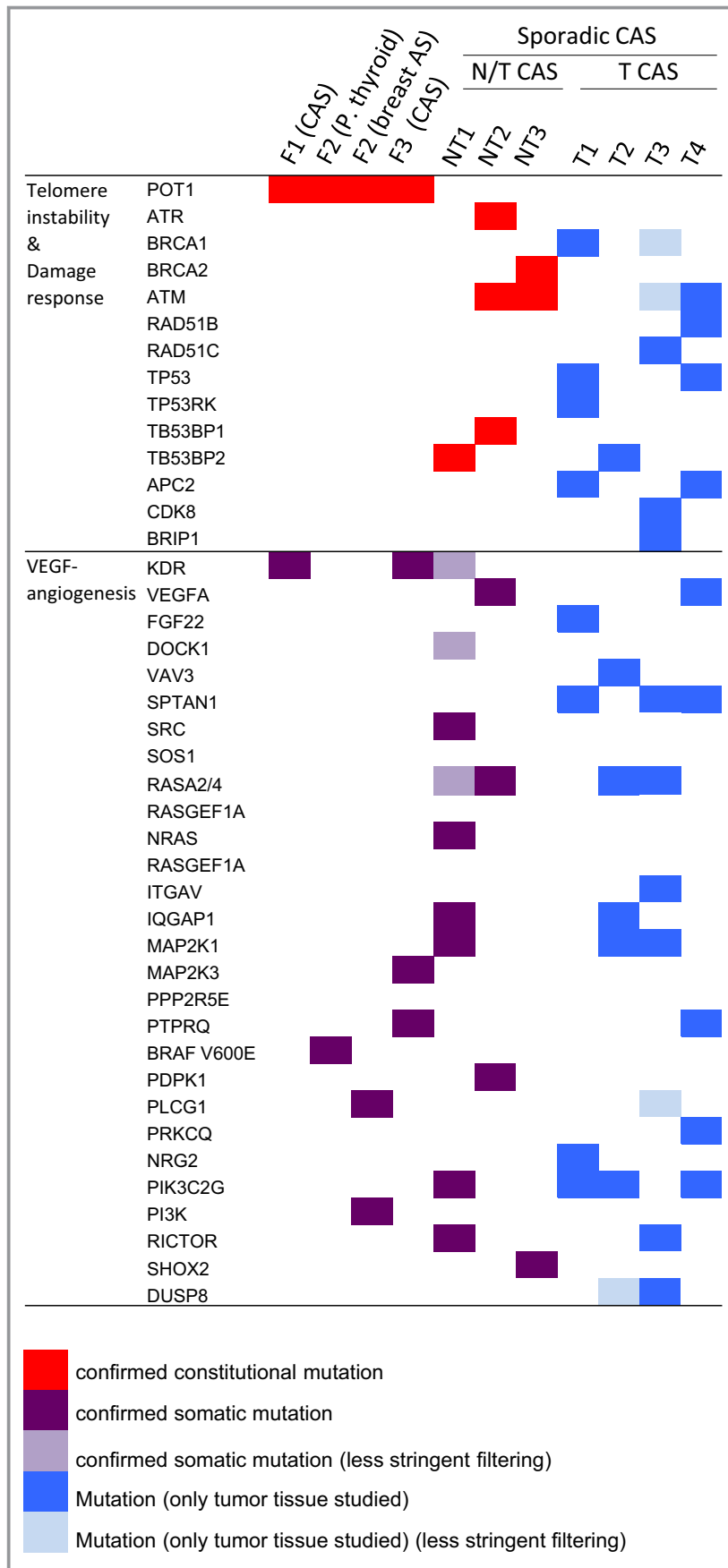
Figure 3. VEGF (vascular endothelial growth factor)-angiogenesis signaling and cell cycle regulation pathways. VEGF signaling is a growth factor pathway to stimulate vasculogenesis and angiogenesis. **A**, MAPK/ERK signaling regulates cell proliferation. **B**, AKT/PI3K signaling is related to protein synthesis and cell cycle signaling. Locations of anti-P-ERK and anti-P-S6 used in IHC studies are also shown in the pathway (white arrows). **C**, Damage-signaling pathway. AKT/PI3K signaling inhibits apoptosis, senescence, and cell cycle arrest through inhibition of FOXO, which in turn positively regulates p21 and p27 activity.

BRAF p.Val600Glu and *PIK3CA* p.Arg88Gln mutations have been described as activators of the angiogenic response.^{31,32} The somatic mutation *BRAF* p.Val600Glu has also been reported in gliomas³³ and melanomas,³⁴ where constitutional mutations in the *POT1* gene were also described.¹⁰⁻¹² In summary, individuals with nonfunctional *POT1* did not repress damage signaling (ATR) and showed a constitutive increase of p21 and p27 expression, which is in agreement with cell cycle arrest. In addition, somatic activating mutations in the angiogenesis pathway were acquired. Interestingly, activating somatic mutations in the *KDR* gene were found in both studied patients affected with CAS and carrying a *POT1* germline mutation (F1 and F3). This was also observed in other tissues and tumors different from cardiac angiosarcomas with mutations in the *POT1* gene (thyroid and breast from patient F2), demonstrating that not only in cardiac tissue is there a strong correlation between constitutional senescence mediated by *POT1* malfunction and the acquisition of somatic mutations in the angiogenesis pathway.

Sporadic Cardiac Angiosarcomas Without *POT1* Mutations

Although in 4 of the 10 patients studied no discrimination between germline and somatic mutations could be made, mutations in the pathways that were affected by the mutation in the *POT1* gene at both the constitutional and the somatic level were also found in these patients.

Studied CAS individuals without constitutional mutations in the *POT1* gene presented mutations in genes that were involved in damage response signaling (ATM-ATR-TP53) (Figure 4). IHC studies with anti-p21 and anti-p27 antibodies confirmed the damage response activation in all sporadic CAS individuals (Table 1 and Figure 2). Therefore, our results suggest a relation between telomere instability (familial CAS) and altered damage signaling (sporadic CAS) on 1 hand, and increased cell cycle arrest leading to the cessation of cell division on the other. Our observation is in agreement with previous studies in which overexpression of TP53 was detected by immunohistochemistry in 49% of angiosarcoma



Downloaded from <http://ahajournals.org> by on September 24, 2019

Figure 4. Genes with mutations in the studied CAS individuals. Genes are distributed considering the gene ontology among telomere instability and damage response or VEGF (vascular endothelial growth factor)-angiogenesis signaling pathways. Exomes from normal/tumor tissues of 3 patients (F1, F2, and F3) carrying the constitutional *POT1* p.Arg117Cys mutation (orange) and 3 sporadic CAS individuals not carrying mutations in the *POT1* gene (NT1, NT2, and NT3) were sequenced. Constitutional mutations refer to variants found in blood samples and found in common in both N and T tissues (red). Mutations found only in tumor tissue were considered somatic (purple). Only tumor tissue from another 4 sporadic CAS individuals (T1 to T4) was also sequenced. A distinction between first event and somatic variants could not be made for the mutations found in these individuals (blue). Less stringent frequency filtering corresponds to a minor allele frequency <0.05 (light purple) instead of <0.01 (light blue). AS indicates angiosarcoma; CAS, cardiac angiosarcoma; N, normal tissue; P, thyroid, papillary thyroid tumor; T, tumor tissue.

patients.¹⁹ Somatic activating mutations in the VEGF-angiogenesis pathway were also found in tumor tissue of all sporadic CAS individuals (Figures 2 and 4). Similar studies performed in angiosarcomas also uncovered somatic driver mutations in the VEGF/PLCG1 angiogenesis pathway.^{18,20,21}

Constitutional Cell Cycle Arrest May Fuel the Acquisition of Somatic Mutations in the Angiogenesis Pathway in Angiosarcomas

Activation of damage signaling in both familial (*POT1* mutations carriers) and sporadic angiosarcomas (ATM-ATR-TP53 mutation carriers) induced constitutional senescence and reduced cell division (Figure 2). Our results strongly suggest a correlation between constitutional cell cycle arrest and the acquired somatic mutations in the VEGF-angiogenesis pathway that drive angiosarcoma formation. Moreover, increased cell cycle arrest due to *POT1* malfunction also uncovered somatic angiogenesis activation in tumors other than cardiac angiosarcomas. Damage response signaling and the VEGF-signaling pathway are mutually regulated (Figure 3). Recently, telomere biology and the PI3K pathway (angiogenesis) were also shown to be functionally connected, and phosphorylation activity of the PI3K/AKT pathway was demonstrated to affect telomere stability in vitro.³⁵ In vitro studies with stem cells from *Pot1a* knockout mice with increased telomere dysfunction also suggested a correlation with increased proliferation.³⁶ Our results indicate that the observed cell cycle deregulation may interfere with apoptosis. This bypass of apoptosis would permit the acquisition of somatic mutations. In addition, cells carrying somatic mutations in genes involved in attenuating cell cycle arrest, which depletes progenitor stem cells in nontumor tissues, may undergo positive selection. A bypass of apoptosis was also suggested in studies in which *POT1* was inactivated in vitro, and induced genomic instability enabled cancer cells to acquire additional mutations and conferred aggressive behavior. Attenuation of the damage response was suggested to allow tumor cells to

bypass the proliferation defect imposed by *POT1* inhibition.³⁶ Therefore, under senescence conditions, activating somatic mutations in the angiogenesis pathway would acquire an important role to replenish the depleted tissue. However, the mutations found in the angiogenesis pathway would contribute to angiosarcoma formation and progression.

Clinical Significance of the Identified Mechanism

Activation of the VEGF-angiogenesis pathway was found in all studied individuals with AS (familial and sporadic). However, our IHC studies revealed 2 different staining patterns that correlated with the location of the somatic mutations (Figure 2). Tumors with mutations in the AKT-PI3K signaling pathway (F1, F2, F3, and T1) were only positively stained with the anti-P-S6 antibody (Table 1 and Figure 4). The individuals with mutations only in the MAPK/ERK signaling pathway (NT1, NT2 and the papillary thyroid tumor of F2) or in both molecular signaling pathways (T3 and T4) were positively stained with both antibodies (Table 1). Therefore, different somatic alterations regarding increased angiogenesis may occur in response to senescence. These results give important clues regarding the diagnosis and classification of angiosarcomas.

Our results also have an important clinical relevance regarding treatment and translational research. Inhibition of angiogenesis may be useful to stop tumor progression.³⁷ However, angiogenesis inhibition would mitigate the effect of the driving somatic mutations but would not revert cell cycle arrest or the suggested bypass of apoptosis and would therefore not curtail the acquisition of new somatic mutations. Treatment with PI3K inhibitors of patient-derived xenografts also showed increased telomeric DNA damage.³⁵ Our results suggest that further studies regarding ATM/ATR, damage signaling and cell cycle inhibition activity might lead to recovering cell cycle control and preventing the acquisition of somatic mutations, including in asymptomatic patients carrying *POT1* mutations. Regarding this issue, the second

sequencing experiment with the IBM Watson platform also pointed to the damage-signaling pathway as a therapeutic target. Actionable variants in the *TP53* gene were highlighted in both studied CAS individuals (T1 and T4). Therefore, although somatic driver variants were found to occur in the angiogenesis pathway, only damage response signaling was found actionable for both studied angiosarcomas (Tables S4 and S5).

In summary, our current results demonstrate that inhibition of *POT1* gene function and damage response malfunction both activate ATR-dependent DNA damage signaling, which increases cell cycle arrest that would diminish cell proliferation in constitutional tissue, and that triggers somatic activating mutations in the angiogenesis pathway in angiosarcomas. Interestingly, our results and the 2 previously studied CAS patients^{16,17} suggest a strong correlation between constitutional mutations in the *POT1* gene, somatic activating mutations in the *KDR* gene, and CAS development. Importantly, the same mechanism was observed in tumor types different from cardiac tumors for patients carrying *POT1* mutations and long telomeres (Figure 2). The significance of this mechanism needs to be further evaluated, and it is conceivable that *POT1* mutations lead to the same acquired somatic alterations in other tissues and tumor types such as glioma, melanoma, or colorectal cancer.⁷ Therefore, mutations found in the *POT1* gene and other genes involved in DNA damage-response signaling (*ATR/ATM* and *TP53*) in the studied cardiac angiosarcomas correlate with constitutional cell cycle arrest, which would deplete the progenitor cells and trigger tissue stress. This tissue stress would give rise to a bypass of the apoptotic regulation, which permits the acquisition of multiple somatic events. In all studied CAS cases (patients with familial CAS carrying the *POT1* mutation and patients with sporadic CAS), somatic activating mutations were found in the angiogenesis pathway, which drives tumor formation. At a translational level, inhibition of angiogenesis might be useful to halt tumor progression. However, inhibition of angiogenesis would not reverse cell cycle arrest or the suggested bypass of apoptosis in constitutional asymptomatic tissue. Instead, the use of ATM/ATR activity inhibitors might restore cell cycle control and prevent the acquisition of somatic mutations.

Acknowledgments

We are grateful to Dr Manuel Serrano from the Tumour Suppression Group (CNIO) for critical revision of the manuscript. We want to acknowledge the patients and the BioBank of the Complejo Hospitalario Universitario de Santiago (CHUS) (PT17/0015/0002), integrated into the Spanish National Biobanks Network, for their collaboration and Centro Nacional de Análisis Genómico (CNAG) for the technical support with WES data.

Sources of Funding

Benitez's laboratory is partially funded by Centro de Investigación (CIBERER), Horizon2020 BRIDGES project, and by the Spanish Ministry of Health supported by Federación Española de Enfermedades Raras (FEDER) funds (PI16/00440). Garcia-Pavia's group is partially supported by the Instituto de Salud Carlos III (ISCIII) (grants CB16/11/00432 and PI14/0967) and by the Spanish Ministry of Economy and Competitiveness (grant SAF2015-71863-REDT). Garcia-Pavia's and Crespo-Leiro's groups are supported by FEDER funds. Urioste's laboratory is funded by Spanish Ministry of Health supported by FEDER fund (PI14/00459).

Disclosures

None.

References

- Malkin D. Li-Fraumeni syndrome. *Genes Cancer*. 2011;2:475–484.
- Butany J, Nair V, Naseemuddin A, Nair GM, Catton C, Yau T. Cardiac tumours: diagnosis and management. *Lancet Oncol*. 2005;6:219–228.
- Patel SD, Peterson A, Bartczak A, Lee S, Chojnowski S, Gajewski P, Loukas M. Primary cardiac angiosarcoma—a review. *Med Sci Monit*. 2014;20:103–109.
- Casha AR, Davidson LA, Roberts P, Nair RU. Familial angiosarcoma of the heart. *J Thorac Cardiovasc Surg*. 2002;124:392–394.
- Keeling IM, Ploner F, Rigler B. Familial cardiac angiosarcoma. *Ann Thorac Surg*. 2006;82:1576.
- Calvete O, Martinez P, Garcia-Pavia P, Benitez-Buelga C, Paumard-Hernández B, Fernandez V, Dominguez F, Salas C, Romero-Laorden N, Garcia-Donas J, Carrillo J, Perona R, Triviño JC, Andrés R, Cano JM, Rivera B, Alonso-Pulpon L, Setien F, Esteller M, Rodriguez-Perales S, Bougeard G, Frebourg T, Urioste M, Blasco MA, Benítez J. A mutation in the *POT1* gene is responsible for cardiac angiosarcoma in TP53-negative Li-Fraumeni-like families. *Nat Commun*. 2015;6:8383.
- Calvete O, Garcia-Pavia P, Domínguez F, Bougeard G, Kunze K, Braeuning A, Teule A, Lasa A, Ramón y Cajal T, Llorca G, Fernández V, Lázaro C, Urioste M, Benitez J. The wide spectrum of *POT1* gene variants correlates with multiple cancer types. *Eur J Hum Genet*. 2017;25:1278–1281.
- Speedy HE, Kinnersley B, Chubb D, Broderick P, Law PJ, Litchfield K, Jayne S, Dyer MJS, Dearden C, Follows GA, Catovsky D, Houlston RS. Germline mutations in shelterin complex genes are associated with familial chronic lymphocytic leukemia. *Blood*. 2016;128:2319–2326.
- Chubb D, Broderick P, Dobbins SE, Frampton M, Kinnersley B, Penegar S, Price A, Ma YP, Sherborne AL, Palles C, Timofeeva MN, Bishop DT, Dunlop MG, Tomlinson I, Houlston RS. Rare disruptive mutations and their contribution to the heritable risk of colorectal cancer. *Nat Commun*. 2016;7:11883.
- Bainbridge MN, Armstrong GN, Gramatges MM, Bertuch AA, Jhangiani SN, Doddapaneni H, Lewis L, Tombrello J, Tsavachidis S, Liu Y, Jalali A, Plon SE, Lau CC, Parsons DW, Claus EB, Barnholtz-Sloan J, Il'yasova D, Schildkraut J, Ali-Osman F, Sadetzki S, Johansen C, Houlston RS, Jenkins RB, Lachance D, Olson SH, Bernstein JL, Merrell RT, Wrensch MR, Walsh KM, Davis FG, Lai R, Shete S, Aldape K, Amos CI, Thompson PA, Muzny DM, Gibbs RA, Melin BS, Bondy ML. Germline mutations in shelterin complex genes are associated with familial glioma. *J Natl Cancer Inst*. 2014;107:384.
- Robles-Espinoza CD, Harland M, Ramsay AJ, Aoude LG, Quesada V, Ding Z, Pooley KA, Pritchard AL, Tiffen JC, Petljak M, Palmer JM, Symmons J, Johansson P, Stark MS, Gartside MG, Snowden H, Montgomery GW, Martin NG, Liu JZ, Choi J, Makowski M, Brown KM, Dunning AM, Keane TM, López-Otin C, Gruis NA, Hayward NK, Bishop DT, Newton-Bishop JA, Adams DJ. *POT1* loss-of-function variants predispose to familial melanoma. *Nat Genet*. 2014;46:478–481.
- Shi J, Yang XR, Ballew B, Rotunno M, Calista D, Fargnoli MC, Ghiorzo P, Bressac-de Paillerets B, Nagore E, Avril MF, Caporaso NE, McMaster ML, Cullen M, Wang Z, Zhang X, Bruno W, Pastorino L, Queirolo P, Banuls-Roca J, Garcia-Casado Z, Vaysse A, Mohamdi H, Riazalhosseini Y, Foglio M, Jouenne F, Hua X, Hyland PL, Yin J, Vallabhaneni H, Chai W, Minghetti P, Pellegrini C,

- Ravichandran S, Eggermont A, Lathrop M, Peris K, Scarra GB, Landi G, Savage SA, Sampson JN, He J, Yeager M, Goldin LR, Demenais F, Chanock SJ, Tucker MA, Goldstein AM, Liu Y, Landi MT. Rare missense variants in *POT1* predispose to familial cutaneous malignant melanoma. *Nat Genet*. 2014;46:482–486.
13. Maciejowski J, de Lange T. Telomeres in cancer: tumour suppression and genome instability. *Nat Rev Mol Cell Biol*. 2017;18:175–186.
 14. Martínez P, Blasco MA. Telomere-driven diseases and telomere-targeting therapies. *J Cell Biol*. 2017;216:875–887.
 15. Palm W, de Lange T. How shelterin protects mammalian telomeres. *Annu Rev Genet*. 2008;42:301–334.
 16. Kunze K, Spieker T, Gamedinger U, Nau K, Berger J, Dreyer T, Sindermann JR, Hoffmeier A, Gattenlöhner S, Bräuninger A. A recurrent activating *PLCG1* mutation in cardiac angiosarcomas increases apoptosis resistance and invasiveness of endothelial cells. *Cancer Res*. 2014;74:6173–6183.
 17. Zhrebek L, Cherni I, Gross LM, Hinshelwood MM, Reese M, Aldrich J, Guileyardo JM, Roberts WC, Craig D, Von Hoff DD, Mennel RG, Carpten JD. Case report: whole exome sequencing of primary cardiac angiosarcoma highlights potential for targeted therapies. *BMC Cancer*. 2017;17:17.
 18. Lahat G, Dhuka AR, Halleivi H, Xiao L, Zou C, Smith KD, Phung TL, Pollock RE, Benjamin R, Hunt KK, Lazar AJ, Lev D. Angiosarcoma: clinical and molecular insights. *Ann Surg*. 2010;251:1098–1106.
 19. Italiano A, Chen CL, Thomas R, Breen M, Bonnet F, Sevenet N, Longy M, Maki RG, Coindre JM, Antonescu CR. Alterations of the p53 and PIK3CA/AKT/mTOR pathways in angiosarcomas: a pattern distinct from other sarcomas with complex genomics. *Cancer*. 2012;118:5878–5887.
 20. Antonescu CR, Yoshida A, Guo T, Chang NE, Zhang L, Agaram NP, Qin LX, Brennan MF, Singer S, Maki RG. KDR activating mutations in human angiosarcomas are sensitive to specific kinase inhibitors. *Cancer Res*. 2009;69:7175–7179.
 21. Behjati S, Tarpey PS, Sheldon H, Martincorena I, Van Loo P, Gundem G, Wedge DC, Ramakrishna M, Cooke SL, Pillay N, Vollan HKM, Papaemmanuil E, Koss H, Bunney TD, Hardy C, Joseph OR, Martin S, Mudie L, Butler A, Teague JW, Patil M, Steers G, Cao Y, Gumbs C, Ingram D, Lazar AJ, Little L, Mahadeshwar H, Protopopov A, Al Sanna GA, Seth S, Song X, Tang J, Zhang J, Ravi V, Torres KE, Khatri B, Halai D, Roxanis I, Baumhoer D, Tirabosco R, Amary MF, Boshoff C, McDermott U, Katan M, Stratton MR, Futreal PA, Flanagan AM, Harris A, Campbell PJ. Recurrent *PTPRB* and *PLCG1* mutations in angiosarcoma. *Nat Genet*. 2014;46:376–379.
 22. Li H, Durbin R. Fast and accurate long-read alignment with Burrows-Wheeler transform. *Bioinformatics*. 2010;26:589–595.
 23. Richards S, Aziz N, Bale S, Bick D, Das S, Gastier-Foster J, Grody WW, Hegde M, Lyon E, Spector E, Voelkerding K, Rehml HL. Standards and guidelines for the interpretation of sequence variants: a joint consensus recommendation of the American College of Medical Genetics and Genomics and the Association for Molecular Pathology. *Genet Med*. 2015;17:405–424.
 24. McLaren W, Pritchard B, Rios D, Chen Y, Flicek P, Cunningham F. Deriving the consequences of genomic variants with the Ensembl API and SNP Effect Predictor. *Bioinformatics*. 2010;26:2069–2070.
 25. Kamburov A, Stelzl U, Lehrach H, Herwig R. The ConsensusPathDB interaction database: 2013 update. *Nucleic Acids Res*. 2013;41:793–800.
 26. Bachman KE, Argani P, Samuels Y, Silliman N, Ptak J, Szabo S, Konishi H, Karakas B, Blair BG, Lin C, Peters BA, Velculescu VE, Park BH. The *PIK3CA* gene is mutated with high frequency in human breast cancers. *Cancer Biol Ther*. 2004;3:772–775.
 27. Gorenne I, Kavurma M, Scott S, Bennett M. Vascular smooth muscle cell senescence in atherosclerosis. *Cardiovasc Res*. 2006;72:9–17.
 28. Wong LSM, Oeseburg H, De Boer RA, Van Gilst WH, Van Veldhuisen DJ, Van Der Harst P. Telomere biology in cardiovascular disease: the *TERC*^{-/-} mouse as a model for heart failure and ageing. *Cardiovasc Res*. 2009;81:244–252.
 29. Megquier K, Turner-Maier J, Swofford R, Kim J-H, Sarver AL, Wang C, Sakthikumar S, Johnson J, Koltoukian M, Lewellen M, Scott MC, Graef AJ, Borst L, Tonomura N, Alfoldi J, Painter C, Thomas R, Karlsson EK, Breen M, Modiano JF, Elvers I, Lindblad-Toh K. Genomic analysis reveals shared genes and pathways in human and canine angiosarcoma. *bioRxiv*. Available at: <https://www.biorxiv.org/content/biorxiv/early/2019/03/15/570879.full.pdf>. Accessed March 8, 2019.
 30. Kimura ET, Nikiforova MN, Zhu Z, Knauf JA, Nikiforov YE, Fagin JA. High prevalence of *BRAF* mutations in thyroid cancer: genetic evidence for constitutive activation of the *RET*/*PTC*-*RAS*-*BRAF* signaling pathway in papillary thyroid carcinoma. *Cancer Res*. 2003;63:1454–1457.
 31. Bottos A, Martini M, Di Nicolantonio F, Comunanza V, Maione F, Minassi A, Appendino G, Bussolino F, Bardelli A. Targeting oncogenic serine/threonine-protein kinase *BRAF* in cancer cells inhibits angiogenesis and abrogates hypoxia. *Proc Natl Acad Sci USA*. 2012;109:353–359.
 32. Pratilas CA, Xing F, Solit DB. Targeting oncogenic *BRAF* in human cancer. *Curr Top Microbiol Immunol*. 2012;355:83–98.
 33. Penman CL, Faulkner C, Lowis SP, Kurian KM. Current understanding of *BRAF* alterations in diagnosis, prognosis, and therapeutic targeting in pediatric low-grade gliomas. *Front Oncol*. 2015;5:54.
 34. Carlino MS, Long GV, Kefford RF, Rizos H. Targeting oncogenic *BRAF* and aberrant *MAPK* activation in the treatment of cutaneous melanoma. *Crit Rev Oncol Hematol*. 2015;96:385–398.
 35. Méndez-Pertuz M, Martínez P, Blanco-Aparicio C, Gómez-Casero E, Belén García A, Martínez-Torrecuadrada J, Palafox M, Cortés J, Serra V, Pastor J, Blasco MA. Modulation of telomere protection by the *PI3K/AKT* pathway. *Nat Commun*. 2017;8:1278.
 36. Pinzaru AM, Hom RA, Beal A, Phillips AF, Ni E, Cardozo T, Nair N, Choi J, Wuttke DS, Sfeir A, Denchi EL. Telomere replication stress induced by *POT1* inactivation accelerates tumorigenesis. *Cell Rep*. 2016;15:2170–2184.
 37. Maj E, Papiernik D, Wietrzyk J. Antiangiogenic cancer treatment: the great discovery and greater complexity (review). *Int J Oncol*. 2016;49:1773–1784.

SUPPLEMENTAL MATERIAL

Table S1. Filtered somatic variants found in the WES of *POT1* p.Arg117Cys carriers, one CAS and one breast AS with papillary thyroid cancer.

Genes previously shown to be involved in the corresponding pathology are highlighted in grey.

Pathology	Chr	Gene	Position	REF	ALT	ALT allele fraction	Amino acid change	dbSNP	Cosmic	GMAF	ExAC
CAS	1	<i>TMEM52</i>	1850627	CAGCGGCAGG	C	0.224	L26del		COSM1167507	-	-
	1	<i>RCC1</i>	28858834	G	A	0.184	G169Asp	-		-	-
	1	<i>CELSR2</i>	109792751	T	C	0.432	L17P	rs20027726 5	COSM1200708	-	-
	1	<i>NOTCH2</i>	120612234	G	C	0.234	-	-		-	-
	1	<i>NOTCH2NL</i>	145248838	A	G	0.232	-	rs20120485 4		-	-
	1	<i>ARNT</i>	150849103	C	A	0.165	-	rs10305649		0.0289	0.05
	1	<i>LOR</i>	153233990	T	G	0.212	Y189D	-		-	-
	2	<i>NRXN1</i>	50765449	C	T	0.346	W735*	-		-	-
	2	<i>ANKRD36</i>	97820478	G	A	0.432	c.1260+3D	rs79756591	COSM1632174, COSM1632175	-	-
	2	<i>RABL2A</i>	114386168	C	T	0.218	-	-		-	-
	2	<i>HS6ST1</i>	129075877	G	T	0.214	D87E	-		-	-
	2	<i>HS6ST1</i>	129075939	T	A	0.168	K67*	rs20224738 7	COSM1129578	-	-
	2	<i>HOXD11</i>	176972061	G	C	0.344	-	-		-	-
	2	<i>SPATA3</i>	231861032	TCAGCAGCCT AGCCCTGAAT CCACACCA	T	0.188	Q30_Q38del	rs72362780	COSM1406147	-	-
	2	<i>NGEF</i>	233748132	C	T	0.234	R549H	-		-	-
	3	<i>FANCD2</i>	10088266	G	T	0.434	c.1137G>T+3D	rs72492997		-	-
	4	<i>KDR</i>	55968550	CATT	C	0.424	N704del	-		-	-
4	<i>ALB</i>	74280882	G	A	0.546	V397M	-		-	-	
4	<i>DSPP</i>	88537069	T	TGATA GCAGC	0.288	S1085_insDSS	-		-	-	

4	<i>CENPE</i>	104119549	G	C	0.212	-	-	-	-	
4	<i>SYNPO2</i>	119951749	C	T	0.188	R607*	-	-	-	
4	<i>CBR4</i>	169931326	CA	C	0.434	-	rs67305871	-	-	
6	<i>ATAT1</i>	30595639	G	C	0.465	G79A	-	-	-	
6	<i>HLA-DRB5</i>	32497905	G	A	0.365	R33*	rs71549219	-	-	
6	<i>HBS1L</i>	135290447	T	G	0.345	E609D	-	-	-	
7	<i>ZAN</i>	100385561	GGCTTCAGCT ACCGCTTGCA AGGCCGCATG ACCTAT	G	0.208	F2344SfsTer10	rs72364644	COSM1329481, COSM1329482, COSM1329483	-	-
7	<i>TRBV5-5</i>	142148969	A	T	0.498	L101*	-	-	-	
10	<i>ARMC4</i>	28250610	C	A	0.370	D425Y	-	-	-	
10	<i>FGFR2</i>	123325217	C	T	0.430	c.111-1	-	-	-	
11	<i>MUC6</i>	1030228	A	C	0.708	C334G	rs20098033 0	COSM1603961, COSM1603962	-	-
11	<i>CLCF1</i>	67141148	AT	A	0.278	-	-	-	-	
11	<i>PDE2A</i>	72301235	CGT	C	0.234	Y252SfsTer74	-	-	-	
12	<i>DDX11</i>	31237978	C	T	0.188	R186W	rs74087925	-	-	
12	<i>PRKAG1</i>	49397570	C	A	0.234	V234F	-	-	-	
12	<i>KMT2D</i>	49434325	G	A	0.436	R2410*	-	COSM144609, COSM1299436	-	-
12	<i>KMT2D</i>	49444088	GGA	G	0.298	L1094PfsTer20	-	-	-	
14	<i>ZFP36L1</i>	69256806	T	G	0.436	K154T	-	-	-	
16	<i>TOX3</i>	52484238	G	A	0.186	Q31L	-	-	-	
16	<i>PSMB10</i>	67970188	G	C	0.688	R58G	-	COSM139019	-	-
17	<i>SHPK</i>	3524660	CGGCGAT	C	0.444	II30_Al31del	-	-	-	
19	<i>RHPN2</i>	33490566	T	C	0.212	Q384R	-	-	-	
19	<i>RHPN2</i>	33490585	G	A	0.388	Q378*	rs78615454	COSM1318333	-	-
22	<i>POTEH</i>	16287784	C	T	0.268	W34*	rs20037519 0	-	0.006	-
22	<i>SRRD</i>	26879946	GGAGGCGGC	G	0.160	Al33_A39del	rs66831137	-	-	-

				GCCCCGGGGG AGA							
	X	<i>SLC25A5</i>	118604444	G	C	0.426	R236P	rs11441358 2	-	-	
Breast AS	3	<i>PIK3CA</i>	178916876	G	A	0.348	R88Q	rs12191328 7	COSM746	-	
	4	<i>TRIM2</i>	154217059	G	A	0.656	V461M			-	<0.0001
	5	<i>EIF4E1B</i>	176070736	G	A	0.655				-	<0.0001
	10	<i>HPSE2</i>	100503738	C	T	0.258	R229H			-	0.00473
	11	<i>TENM4</i>	78516508	G	A	0.288	R670W			-	<0.0001
	11	<i>CBL</i>	119148966	T	G	0.212	C396G		COSM34074	-	
	12	<i>VWF</i>	6103147	T	C	0.214	Y2160C			-	<0.0001
	13	<i>PARP4</i>	25021323	A	G	0.344	I1039T	rs73172125	COSM147647	-	0.347
	13	<i>COL4A2</i>	111160303	C	T	0.256	A1539V			-	<0.0001
	15	<i>CSPG4</i>	75982085	C	T	0.156	E441K	rs79463888	COSM1317754	-	0.15
	20	<i>BPIFB4</i>	31680303	C	A	0.128	P395T			-	
	20	<i>PLCG1</i>	39795452	C	G	0.434	L752V			-	
	20	<i>WFDC8</i>	44180670	G	A	0.344	R241C	rs14756052 2	COSM1027261	-	<0.0001
Papillary Thyroid	3	<i>RASSF1</i>	50369082	C	T	0.212	R227H			-	<0.0001
	6	<i>MDGA1</i>	37606032	C	T	0.234	V909I		COSM1600157	-	<0.0001
	6	<i>ARID1B</i>	157528658	G	A	0.168	R2168Q			-	<0.0001
	7	<i>BRAF</i>	140453136	A	T	0.324	V600E	rs11348802 2	COSM476	-	<0.0001
	17	<i>PIK3R6</i>	8741894	C	T	0.254	R59K			-	

Table S2. Filtered variants found in the WES of F3 patient affected with CAS (*POT1* p.R117C carrier).

Chr	Genomic			REF	ALT	Fraction	HGVS _p	Existing Variation	GMAF
	Gene Symbol	Position	Position						
chr1	KYAT3	88949093	A	T	0.128	ENSP00000260508.4:p.Leu380Gln	rs144984854	0.0006	
chr2	ANKRD36	97211741	G	A	0.436	ENSP00000391950.2:p.Val1157Met	rs10194525		
chr6	HLA-DRB1	32580249	G	C	0.310	ENSP00000353099.5:p.Thr262Arg			
chr10	EEF1AKM	124774782	C	T	0.168	ENSP00000357829.2:p.Ala98Thr	rs199727427	0.0006	
chr13	PARP4	24447185	A	G	0.304	ENSP00000371419.3:p.Ile1039Thr			
chr17	MYH13	10306461	G	A	0.344	ENSP00000404570.3:p.Arg1822Trp	rs116935297	0.007	
chr17	MAP2K3	21300875	G	T	0.456	ENSP00000345083.4:p.Arg94Leu	rs56067280		
chr18	ANKRD30B	14843024	C	G	0.478	ENSP00000351875.4:p.Pro918Ala	rs180690700		
chr19	COLGALT1	17560463	C	G	0.268	ENSP00000252599.3:p.Leu163Val	rs764429704		
chr17		63491216	C	T	0.675	ENSP00000464149.1:p.Thr342Met	rs3730043	0.0034	
chr1	VPS13D	12249234	A	C	0.677	ENSP00000478104.1:p.Gln153His	rs116415833	0.0018	
chr1	FAM131C	16058547	G	A	0.104	ENSP00000364814.4:p.Arg245Trp	rs77667563		
chr1	CROCC	16940041	G	C	0.126	ENSP00000364691.4:p.Asp586His	rs9435714		
chr1	KDF1	26952098	A	G	0.456	ENSP00000319179.5:p.Cys95Arg	rs148853297		
chr1	PPCS	42456962	A	T	0.546	ENSP00000361642.3:p.Arg133Trp	rs199807362		
chr1	IPP	45716925	G	A	0.344	ENSP00000379739.3:p.Arg427Cys	rs142095376	0.0002	
chr1	PODN	53078994	G	A	0.778	ENSP00000308315.5:p.Arg543His	rs61999355	0.003	
chr1	FAM151A	54619889	C	G	0.128	ENSP00000306888.2:p.Lys79Asn	rs114883650	0.0144	
chr1	RBMXL1	88983615	C	G	0.376	ENSP00000446099.1:p.Gly71Ala	rs111779380		
chr1	TSPAN2	115072962	C	G	0.201	ENSP00000358529.2:p.Gly39Arg	rs147800870	0.0004	
chr1	PDE4DIP	149005208	C	T	0.567	ENSP00000358363.4:p.Arg1396Trp	rs2798901		
chr1	FLG2	152351277	G	A	0.234	ENSP00000373370.4:p.Ser2170Phe	rs201200591,COSM896166		
chr1	CRNN	152409620	A	G	0.198	ENSP00000271835.3:p.Ser488Pro			
chr1	GPA33	167068982	C	A	0.304	ENSP00000356842.3:p.Val119Phe	rs72689400	0.0058	

chr1	KIF14	200592110	T	G	0.567	ENSP00000356319.4:p.Lys928Thr	rs150766596	
chr1	PKP1	201322032	G	A	0.436	ENSP00000263946.3:p.Glu489Lys	rs748085816	
							rs142615706,COSM5042798,COSM5042797,COSM5042796,COSM3360727,COSM3360726,COSM3360725	0.0012
chr1	OBSCN	228350867	C	G	0.128	ENSP00000455507.2:p.Arg7072Gly		
chr1	RHOU	228743354	G	A	0.676	ENSP00000355652.3:p.Val131Met		
chr1	EDARADD	236482309	C	T	0.398	ENSP00000335076.4:p.Ser103Phe	rs114632254,CM114961	0.013
chr1	OR2T3	248473745	G	A	0.298	ENSP00000352604.2:p.Cys132Tyr	rs148025314	
chr1	OR2T34	248573866	G	A	0.126	ENSP00000330904.2:p.Arg298Cys	rs148590921	
chr1	OR2T27	248650526	T	C	1.000	ENSP00000342008.3:p.Tyr120Cys		
chr2	MBOAT2	8873294	C	T	0.107	ENSP00000302177.3:p.Val233Ile	rs34573615	0.0142
chr2		47087059	C	A	0.172	ENSP00000408527.2:p.Met232Ile	rs184422124	0.0008
chr2	ASB3	53765485	G	C	0.243	ENSP00000263634.2:p.Leu30Val	rs36020289	0.0056
chr2	TSPYL6	54255416	G	A	0.778	ENSP00000417919.2:p.Arg246Cys	rs17189743	0.0204
chr2	USP34	61278194	G	A	0.166	ENSP00000381577.2:p.Pro1802Ser		
chr2	ANKRD36C	95944662	T	A	0.214	ENSP00000403302.1:p.Asn486Tyr	rs77220524	
chr2	ASTL	96132701	C	T	0.463	ENSP00000343674.2:p.Arg159His	rs61735195	0.0066
chr2	NIFK	121732168	C	T	0.184	ENSP00000285814.4:p.Glu94Lys	rs751855520	
chr2	LCT	135817693	T	A	0.564	ENSP00000264162.2:p.Lys452Met		
chr2	LRP1B	140868259	G	A	0.804	ENSP00000374135.3:p.Leu1392Phe	rs200955532,COSM1007053	
chr2	NMI	151275501	G	A	0.756	ENSP00000243346.5:p.Thr206Met	rs199573903	0.0002
chr2	SLC39A10	195716880	A	G	0.278	ENSP00000386766.3:p.His647Arg	rs755523552	
chr2	TNS1	217882350	A	C	0.674	ENSP00000171887.4:p.Ile311Met	rs11680854	0.0104
chr2	ESPNL	238131340	A	G	0.201	ENSP00000339115.3:p.Lys876Glu	rs149541007	0.0062
chr3	FANCD2	10065867	G	C	0.436	ENSP00000287647.3:p.Cys758Ser	rs540805431	0.0002
chr3	TTC21A	39138609	G	A	0.678	ENSP00000398211.2:p.Glu1291Lys	rs80238762	0.0058
chr3	DNAH1	52360039	G	A	0.322	ENSP00000401514.2:p.Val1511Met	rs61734638	0.0084
chr3	ZNF717	75737092	C	T	0.128	ENSP00000419377.1:p.Cys794Tyr	rs139633377	

chr3	ZNF717	75737101	G	T	0.201	ENSP00000419377.1:p.Pro791His	rs79138891	
chr3	ZNF717	75737127	A	C	0.128	ENSP00000419377.1:p.His782Gln	rs79811623	
chr3	ZNF717	75737622	T	A	0.344	ENSP00000419377.1:p.Arg617Ser	rs76175438	
chr3	ZNF717	75737840	C	T	0.166	ENSP00000419377.1:p.Glu545Lys	rs76496075	
chr3	ZNF717	75738575	G	A	0.236	ENSP00000419377.1:p.Arg300Cys	rs1962893	
chr3	OR5K1	98469710	T	C	0.768	ENSP00000373193.2:p.Leu45Ser	rs200654905	0.003
chr3	BBX	107716685	C	T	0.924	ENSP00000319974.8:p.Arg81Trp	rs142400819	0.003
chr3	ARHGEF26	154225981	C	G	0.440	ENSP00000348828.4:p.Asn687Lys		
chr3	GPR149	154428985	G	C	0.778	ENSP00000374390.2:p.Pro211Ala	rs774089990	
chr3	MUC20	195726080	G	C	0.234	ENSP00000414350.2:p.Asp493His		
chr3	MUC20	195729690	C	G	0.128	ENSP00000414350.2:p.Ser671Cys		
chr3	MUC4	195762138	C	A	1.000	ENSP00000417498.3:p.Ala4821Ser	CM066583	
chr3	MUC4	195789859	G	A	0.184	ENSP00000417498.3:p.Thr574Ile		
chr4	IDUA	987896	C	G	0.134	ENSP00000247933.4:p.His82Gln	rs148775298	0.0012
chr4	HTT	3207344	G	A	0.310	ENSP00000347184.5:p.Gly2047Arg	rs181217572	0.0004
chr4	TLR1	38796634	G	A	0.780	ENSP00000354932.2:p.Pro733Leu	rs5743621	0.0126
chr4	KDR	55098758	G	C	0.654	ENSP00000263923.4:p.Thr771Arg	COSM94566,COSM4381082	
chr4	UGT2B15	68670105	T	G	0.388	ENSP00000341045.5:p.Ser172Arg	rs200638397	0.0002
chr4	RUFY3	70806627	C	G	0.124	ENSP00000370394.3:p.Leu611Val	rs754675264	
chr4	CCSER1	90308466	G	C	0.432	ENSP00000425040.1:p.Ser61Thr	rs184253075	0.0008
chr4	PDLIM5	94455353	A	G	0.567	ENSP00000480359.1:p.Lys22Arg	rs75841704	0.0078
chr4	UNC5C	95170263	C	T	0.128	ENSP00000406022.1:p.Ala841Thr	rs34585936	0.0184
chr4	QRFPR	121380442	A	C	0.214	ENSP00000377948.2:p.Val69Gly	rs34270076	0.0076
chr4	CBR4	169002197	C	A	0.678	ENSP00000303525.3:p.Val137Phe		
chr4	CBR4	169002200	T	A	0.455	ENSP00000303525.3:p.Ile136Phe		
chr4	TLR3	186084674	C	A	0.134	ENSP00000296795.2:p.Ala839Asp	rs201540925,COSM4584973	0.0002
chr5	SLC9A3	488354	C	T	0.436	ENSP00000264938.3:p.Val213Ile	rs143027124	
chr5	C5orf49	7831902	T	G	0.166	ENSP00000382708.2:p.Asn131Thr		

chr5	ADGRV1	90705420	G	A	0.124	ENSP00000384582.2:p.Ala2803Thr	rs111033530	0.0048
chr5	MARCH3	126878360	C	T	0.356	ENSP00000309141.5:p.Arg143Gln	rs138413676	
chr5	LECT2	135951324	C	T	0.304	ENSP00000274507.1:p.Gly63Glu	rs149560293	0.0068
chr5	PCDHGA6	141374360	G	A	0.256	ENSP00000429601.1:p.Glu93Lys	rs200765071	
chr5	PCDH12	141945665	C	T	0.732	ENSP00000231484.3:p.Gly1091Ser	rs779814208	
chr5	SCGB3A2	147881560	G	A	0.652	ENSP00000296694.4:p.Gly57Asp	rs140599638	0.0004
chr5	SLC36A2	151343594	C	A	0.224	ENSP00000334223.4:p.Gly87Val	rs77010315,CM086960	0.005
chr5	GFPT2	180301596	T	C	0.364	ENSP00000253778.8:p.Arg673Gly		
chr6	SOX4	21594616	C	G	0.578	ENSP00000244745.1:p.Leu28Val	rs140231408,COSM3697699	0.0066
chr6	BTN2A2	26392401	G	A	0.576	ENSP00000349143.4:p.Ala336Thr	rs142803339,COSM3745097	0.0092
							CD994645,COSM5446135,COSM5446134,COSM4593407	
chr6	HLA-A	29944253	G	C	0.168	ENSP00000379873.1:p.Asp251His		
chr6	PPP1R10	30609877	C	G	0.222	ENSP00000365694.2:p.Gly23Ala		
chr6	HLA-DRB1	32580779	C	T	0.128	ENSP00000353099.5:p.Ala244Thr	rs3830125	
chr6	HLA-DRB1	32589669	G	C	0.201	ENSP00000353099.5:p.Pro25Arg	rs148093782	
chr6	HLA-DQB2	32757848	T	C	0.344	ENSP00000396330.2:p.Ser228Gly	rs9276572	
chr6	PPIL1	36871822	C	G	0.134	ENSP00000362803.5:p.Cys36Ser	rs12194408	0.0098
chr6	PTK7	43130655	G	A	0.276	ENSP00000418754.1:p.Arg277His	rs78949718	0.0028
chr6	POLR1C	43520104	C	T	0.128	ENSP00000361465.3:p.Arg141Cys	rs148385032	0.0014
chr6	DST	56552557	C	T	0.128	ENSP00000307959.7:p.Gly3155Glu	rs775546048	
chr6	TTK	80035318	C	T	0.166	ENSP00000358813.2:p.Leu609Phe	rs540538876	0.0002
chr6	PNRC1	89081009	C	T	0.124	ENSP00000336931.3:p.Pro39Ser	rs2231267	0.0056
chr6	ARMC2	108953073	C	T	0.278	ENSP00000376417.4:p.Thr546Met	rs61741720	0.0132
chr6	VNN1	132683243	T	C	0.128	ENSP00000356905.4:p.Tyr480Cys	rs567530094	0.0002
chr6	SHPRH	145922832	G	A	0.243	ENSP00000356475.2:p.Arg1184Cys	rs148401398	0.0014
chr7	AMZ1	2709683	G	T	0.376	ENSP00000308149.4:p.Cys272Phe	rs148137749	0.0006
chr7	SDK1	3962743	G	A	0.455	ENSP00000385899.2:p.Gly441Arg	rs139796765	0.0058
chr7	TNRC18	5309293	C	T	0.677	ENSP00000395538.1:p.Gly2822Arg	COSM3881739,COSM3881740	

chr7	PSPH	56021118	T	C	0.295	ENSP00000378854.3:p.Asp32Gly		
chr7	GATAD1	92456449	C	T	0.184	ENSP00000287957.3:p.Arg233Trp	rs34768413	0.007
chr7	FBXO24	100590263	A	C	0.128	ENSP00000416558.2:p.Glu114Asp	rs545357401	0.0002
chr7	POT1	124863547	G	A	0.457	ENSP00000350249.3:p.Arg117Cys	rs780936436	
chr7	CPA2	130289628	C	A	0.335	ENSP00000222481.4:p.Leu381Met	rs146796996	0.0012
chr7	TRBV20-1	142627134	A	T	0.310	ENSP00000374917.3:p.Arg24Trp		
chr7	PRSS1	142750558	C	G	0.436	ENSP00000308720.7:p.Ala15Gly	rs200665515,COSM3723223	
chr7	PRSS1	142750660	G	T	0.567	ENSP00000308720.7:p.Gly49Val	rs138464021	
chr7	PRSS1	142750672	T	A	0.668	ENSP00000308720.7:p.Ile53Asn	rs149246646	
chr7	PRSS1	142752506	G	T	0.574	ENSP00000308720.7:p.Gly177Val		
chr7	SSPO	149802064	C	T	0.256	ENSP00000485256.1:p.Ser2508Phe	rs140977594	0.0056
chr7	KMT2C	152247922	C	T	0.446	ENSP00000262189.6:p.Gly838Ser	COSM4591270	
chr7	KMT2C	152265180	C	T	0.675	ENSP00000262189.6:p.Asp348Asn	rs201834857,COSM228110	
chr7	VIPR2	159031954	C	T	0.788	ENSP00000262178.2:p.Cys362Tyr	rs147214125	0.0004
chr8	SGCZ	14108196	G	A	0.476	ENSP00000371512.1:p.Pro196Leu	rs145213189	0.0004
chr8	PDGFRL	17642653	T	A	0.324	ENSP00000444211.1:p.Ile327Asn	rs35346456	0.0022
chr8	MTUS1	17653257	C	G	0.222	ENSP00000262102.6:p.Glu1105Gln	rs61733705	0.0066
chr8	MTUS1	17684434	T	G	0.166	ENSP00000262102.6:p.Lys911Thr	rs61748836	0.0046
chr8	CYP7A1	58497114	A	G	0.436	ENSP00000301645.3:p.Leu133Pro		
chr8	CSPP1	67116017	C	G	0.657	ENSP00000262210.5:p.Ser459Cys	rs146431326	0.0012
chr8	NBN	89971232	G	A	0.436	ENSP00000265433.3:p.Arg215Trp	rs34767364,CM044022	0.001
chr8	PABPC1	100709584	G	A	0.566	ENSP00000313007.5:p.Arg374Cys	rs200409148	
chr8	PABPC1	100709589	T	C	0.534	ENSP00000313007.5:p.Glu372Gly	rs201076736	
chr8	PABPC1	100709611	C	A	0.128	ENSP00000313007.5:p.Val365Leu	rs202074479	
chr8	PABPC1	100717815	G	C	0.312	ENSP00000313007.5:p.Ala154Gly	rs113614781	
chr8	DEPTOR	119965343	G	C	0.122	ENSP00000286234.5:p.Glu179Asp	rs766410544	
chr8	PHF20L1	132832298	G	A	0.376	ENSP00000378784.2:p.Arg603Gln	rs184113048,COSM1196723,COSM1196724	0.003

chr9	ADAMTSL	18684733	G	T	0.184	ENSP00000369921.4:p.Ala503Ser	rs149221350,COSM3906436,COSM3906437	0.0012
chr9	LINGO2	27949346	A	C	0.345	ENSP00000369328.1:p.Ile442Met		
chr9	SHC3	89042122	G	A	0.304	ENSP00000364995.4:p.Pro422Ser	rs771704230,COSM24411	
chr9	OR13C5	104599179	G	A	0.431	ENSP00000363911.2:p.Pro79Ser	rs7025570,COSM4163183	
chr9	TRIM32	116698344	G	A	0.128	ENSP00000408292.1:p.Arg201His		
chr9	LAMC3	131072789	C	T	0.655	ENSP00000354360.4:p.Ser1124Phe	rs113259170	0.0032
chr9	GBGT1	133153893	C	T	0.756	ENSP00000361110.3:p.Arg243His	rs143563851,COSM4163479	0.001
chr10	CUBN	16890385	G	A	0.678	ENSP00000367064.4:p.Ala2914Val	rs45551835,COSM32707	0.0064
chr10	NPY4R	46462341	C	A	0.234	ENSP00000363431.1:p.Ala99Ser		
chr10	GPRIN2	46549695	C	A	0.112	ENSP00000363436.1:p.Val348Leu	rs4926046	
chr10	GPRIN2	46550133	C	A	0.324	ENSP00000363436.1:p.Gly202Trp	rs11204658	
chr10	GPRIN2	46550598	C	T	0.436	ENSP00000363436.1:p.Val47Met		
chr10	GPRIN2	46550622	G	C	0.234	ENSP00000363436.1:p.Leu39Val		
chr10	LHPP	124517198	G	A	0.536	ENSP00000357835.5:p.Asp215Asn	rs140823928	0.0038
chr10	CTBP2	124994530	G	A	0.598	ENSP00000311825.6:p.Ser780Phe	rs374871777,COSM2021369,COSM2021368	
chr10	CTBP2	124994542	C	T	0.504	ENSP00000311825.6:p.Ser776Asn	rs78155918	
chr10	CTBP2	124994563	A	T	0.544	ENSP00000311825.6:p.Leu769Gln	rs150320719	
chr10	CTBP2	124994577	C	A	0.657	ENSP00000311825.6:p.Gln764His	rs80025996,COSM5764564,COSM5764563	
chr10	CTBP2	125002983	T	G	0.346	ENSP00000311825.6:p.Asp652Ala	rs796433756	
chr10	CTBP2	125003006	T	C	0.310	ENSP00000311825.6:p.Ile644Met	rs112239066	
chr10	CTBP2	125003010	C	T	0.215	ENSP00000311825.6:p.Arg643Gln	rs760489730,COSM5620576,COSM5620575	
chr10	CTBP2	125003036	C	A	0.166	ENSP00000311825.6:p.Lys634Asn	rs201760950,COSM4441587,COSM4441586	
chr10	CTBP2	125003065	T	A	0.184	ENSP00000311825.6:p.Ile625Phe	rs75794788,COSM4144456,COSM4144455	
chr10	CTBP2	125003091	G	A	0.345	ENSP00000311825.6:p.Ala616Val	rs3198935	
chr10	CTBP2	125003357	G	A	0.128	ENSP00000311825.6:p.Thr605Met	rs768573864,COSM2021395,COSM2021394	
chr10	CTBP2	125003368	G	C	0.267	ENSP00000311825.6:p.Asp601Glu	rs1058301,COSM5763526,COSM5763525,COSM4675296,COSM4675295	

chr10	CTBP2	125003410	C	G	0.215	ENSP00000311825.6:p.Glu587Asp	rs74705267,COSM4144460,COSM4144459	
chr10	CTBP2	125003448	G	C	0.166	ENSP00000311825.6:p.Leu575Val	rs3198920	
chr10	CTBP2	125003450	G	A	0.376	ENSP00000311825.6:p.Pro574Leu	rs796256730,COSM5620578,COSM5620577	
chr10	CTBP2	125003460	G	T	0.435	ENSP00000311825.6:p.His571Asn	rs796388243	
chr10	CTBP2	125003466	G	T	0.243	ENSP00000311825.6:p.Pro569Thr		
chr10	CTBP2	125003468	C	A	0.213	ENSP00000311825.6:p.Gly568Val	rs368195398	
chr10	CTBP2	125003470	G	T	0.178	ENSP00000311825.6:p.Asn567Lys	rs797010536	
chr11	MUC6	1016961	G	A	0.166	ENSP00000406861.2:p.Thr1947Ile	rs773824783	
chr11	MUC6	1017069	G	A	0.801	ENSP00000406861.2:p.Thr1911Met	rs80333708	
chr11	MUC6	1017135	G	A	0.726	ENSP00000406861.2:p.Thr1889Ile	rs747429892	
chr11	MUC6	1017183	G	T	0.405	ENSP00000406861.2:p.Pro1873Gln	rs34844844	0.0004
chr11	MUC6	1017337	T	C	0.435	ENSP00000406861.2:p.Thr1822Ala	rs76686156	
chr11	MUC6	1018042	A	G	0.235	ENSP00000406861.2:p.Ser1587Pro	rs200364398	
chr11	MUC6	1018473	A	T	0.387	ENSP00000406861.2:p.Leu1443His	rs112923701	
chr11	OR51J1	5403408	C	T	0.468	ENSP00000332473.1:p.Ser271Phe	rs183738872	0.0008
chr11	SAA2-SAA4	18245916	A	G	0.234	ENSP00000485552.1:p.Val75Ala	rs71469388	
chr11	LRP4	46895950	G	A	0.435	ENSP00000367888.1:p.Arg373Trp	rs118009068	0.0106
chr11	FOLH1	49186715	G	A	0.665	ENSP00000256999.2:p.Arg190Trp	rs75111588	
chr11	OR4C46	54603244	C	T	0.657	ENSP00000329056.1:p.Cys252Tyr	rs11246608	
chr11	OR4C46	54603280	G	A	0.879	ENSP00000329056.1:p.Ser240Phe	rs11246607	
chr11	OR9G1	56700722	A	G	0.342	ENSP00000309012.1:p.Tyr112Cys	rs4990194	0.0056
chr11	OR9G1	56700892	C	T	0.210	ENSP00000309012.1:p.Arg169Cys	rs11228733	0.0008
chr11	OR9G1	56701223	T	A	0.128	ENSP00000309012.1:p.Val279Glu	rs79251113	
chr11	ESRRA	64315848	T	C	0.184	ENSP00000384851.1:p.Leu385Pro	rs201072913	
chr11	ESRRA	64315856	C	T	0.376	ENSP00000384851.1:p.Leu388Phe	rs79204587	
chr11	ESRRA	64315859	C	T	0.435	ENSP00000384851.1:p.Arg389Cys	rs80310817	
chr11	ACTN3	66554587	C	T	0.231	ENSP00000422007.1:p.Pro217Leu	rs370740496	
chr11	NUMA1	72014043	G	A	0.435	ENSP00000377298.3:p.Arg1154Trp	rs61740456	0.001

chr11	USP35	78210302	G	A	0.768	ENSP00000431876.1:p.Arg816His	rs75370284	0.0128
chr11	TRIM49C	90041372	C	A	0.465	ENSP00000388299.1:p.Thr394Asn	rs75119043,COSM3998623,COSM3998622	
chr11	MAML2	96093510	C	T	0.376	ENSP00000434552.1:p.Gly174Asp	rs61749254	0.0042
chr11	SORL1	121496918	G	A	0.346	ENSP00000260197.6:p.Glu270Lys	rs117260922	0.0078
chr11	OR8B2	124382854	G	A	0.567	ENSP00000364152.2:p.Leu164Phe	rs886202	
chr12	WNK1	827047	T	A	0.234	ENSP00000341292.5:p.Leu313Gln		
chr12	FOXMI	2858912	G	A	0.128	ENSP00000342307.2:p.Pro711Leu	rs28919870	0.0044
chr12	CRACR2A	3696811	A	C	0.345	ENSP00000409382.2:p.Asp63Glu	rs144314920	0.0004
chr12	KLRC2	10435931	C	G	0.376	ENSP00000371327.2:p.Arg19Pro	rs75545535	
chr12		10435931	C	G	0.346	ENSP00000437563.1:p.Arg19Pro	rs75545535	
chr12	TAS2R19	11021703	A	G	0.205	ENSP00000375091.2:p.Phe290Ser		
chr12	TAS2R19	11021868	A	C	0.346	ENSP00000375091.2:p.Leu235Arg	rs763119571	
chr12	TAS2R31	11030522	G	A	0.145	ENSP00000375093.2:p.Pro272Ser	rs763119976	
chr12	TAS2R31	11031043	A	G	0.754	ENSP00000375093.2:p.Leu98Pro	rs73049067	
chr12	TAS2R31	11031194	G	C	0.304	ENSP00000375093.2:p.Leu48Val	rs760444623	
chr12	TAS2R30	11134103	G	C	0.166	ENSP00000444736.1:p.Leu48Val	rs113026132	
chr12	PTPRO	15503912	C	G	0.456	ENSP00000281171.4:p.Asn370Lys	rs61754411	0.009
chr12	CCDC65	48918345	A	G	0.345	ENSP00000312706.4:p.Gln227Arg	rs149640178	0.0004
chr12	TROAP	49331358	G	A	0.545	ENSP00000257909.3:p.Arg748Gln	rs200487146,COSM4921428	0.0006
							rs62638191,CM991095,RISN_RDH5:c	
chr12	RDH5	55724028	G	T	0.787	ENSP00000257895.5:p.Gly238Trp	.712G>T	0.0004
chr12	MDM1	68332236	G	C	0.456	ENSP00000302537.7:p.Arg4Gly	rs199537908	
chr12	LRR1Q1	85153046	A	C	0.476	ENSP00000376910.2:p.Asp1481Ala	rs191782536	0.0018
chr12	DNAH10	123916480	C	A	0.675	ENSP00000489675.1:p.Asp3464Glu	rs61745785	0.011
chr13	MPHOSPH	19642121	G	T	0.778	ENSP00000355388.4:p.Val74Phe		
chr13	PARP4	24447125	T	C	0.368	ENSP00000371419.3:p.Gln1059Arg	rs77269056	
chr13	PABPC3	25096638	C	T	0.215	ENSP00000281589.3:p.Thr147Ile	rs78432860	
chr13	PABPC3	25096659	C	G	0.567	ENSP00000281589.3:p.Ala154Gly	rs75760907	

chr13	PABPC3	25096889	A	G	0.786	ENSP00000281589.3:p.Lys231Glu	rs78826513	
chr13	PABPC3	25096951	G	T	0.745	ENSP00000281589.3:p.Met251Ile	rs75281454	
chr13	PABPC3	25097154	C	T	0.564	ENSP00000281589.3:p.Thr319Ile	rs80261016	
chr13	PABPC3	25097291	G	T	0.678	ENSP00000281589.3:p.Val365Leu	rs77466429	
chr13	NEK5	52086336	G	A	0.124	ENSP00000347767.4:p.Arg474Cys	rs35465612	0.0042
chr13	SLC10A2	103049340	G	A	0.434	ENSP00000245312.3:p.Pro290Ser	rs56398830,CM952446	0.0074
chr14	WDR89	63599649	A	T	0.376	ENSP00000378399.2:p.Asp98Glu		
chr14	WDR89	63599677	C	T	0.266	ENSP00000378399.2:p.Cys89Tyr	COSM5764373	
chr14	WDR89	63599684	A	G	0.234	ENSP00000378399.2:p.Ser87Pro		
chr14	SYNE2	64130105	C	A	0.340	ENSP00000350719.3:p.Pro4733Thr	rs75568433	0.0028
chr14	VIPAS39	77453359	C	T	0.675	ENSP00000452181.1:p.Val46Met	rs148360332	0.0006
chr14	IGHV4-31	106349457	G	T	0.564	ENSP00000395656.2:p.Pro61Gln	rs77489245	
chr15	NUTM1	34355873	C	A	0.567	ENSP00000444896.1:p.Ser622Tyr		
chr15	TYRO3	41573327	G	T	0.254	ENSP00000263798.3:p.Val669Leu	rs62001448	
chr15	SPATA5L1	45403247	C	G	1.000	ENSP00000305494.6:p.Ser273Cys	rs143453038,COSM4509821	0.01
chr15	SPATA5L1	45403421	G	T	0.654	ENSP00000305494.6:p.Gly331Val		
chr15	SNX1	64136360	G	A	0.435	ENSP00000261889.5:p.Asp466Asn	rs1802376	0.0074
chr15	MYO9A	71968075	T	C	0.675	ENSP00000348349.5:p.His632Arg	rs552840125	0.0002
chr16	RPL3L	1947003	C	T	0.532	ENSP00000268661.7:p.Val262Met	rs113956264	0.0212
chr16	ACSM2A	20465673	G	A	0.345	ENSP00000459451.1:p.Val112Met		
chr16	ACSM3	20775918	T	C	0.546	ENSP00000289416.5:p.Leu100Pro	rs5713	0.004
chr16	OR16-13	33827483	G	T	0.180	ENSP00000474814.1:p.Ala59Ser	rs4077614	
chr16	CES1	55828971	C	A	0.184	ENSP00000353720.3:p.Gly19Val	rs3826190	
chr16	ZNF319	57996752	C	A	0.184	ENSP00000299237.2:p.Arg505Leu	rs149758697,COSM1191791	0.0002
chr16	AARS	70252728	T	A	0.215	ENSP00000261772.7:p.Lys967Met	rs35744709	0.0036
chr16	CLEC18B	74409592	C	T	0.304	ENSP00000341051.5:p.Asp430Asn		
chr16	ZNF469	88437795	G	C	0.128	ENSP00000402343.1:p.Arg3414Thr	rs199528724,COSM1380396	0.0018
chr17	ITGAE	3757758	G	A	0.166	ENSP00000263087.4:p.Thr323Met	rs71366574	0.0164

chr17	CTC1	8232058	G	A	0.678	ENSP00000313759.8:p.Arg744Cys		
chr17	MYH13	10309647	C	G	0.456	ENSP00000404570.3:p.Asp1614His	rs35069886	0.0068
chr17	MAP2K3	21300880	C	T	0.765	ENSP00000345083.4:p.Arg96Trp		
chr17	MAP2K3	21304522	C	T	0.678	ENSP00000345083.4:p.Thr222Met	rs58609466	
chr17	KCNJ12	21415757	G	A	0.234	ENSP00000463778.1:p.Glu139Lys	rs76265595	
chr17	KCNJ12	21415775	G	A	0.345	ENSP00000463778.1:p.Gly145Ser	rs75029097	0.0002
chr17	KCNJ12	21416124	G	A	0.212	ENSP00000463778.1:p.Arg261His	rs77270326	
chr17	KCNJ12	21416127	T	G	0.256	ENSP00000463778.1:p.Ile262Ser	rs76684759	
chr17	KCNJ12	21416474	G	A	0.345	ENSP00000463778.1:p.Glu378Lys	rs78547883	
chr17	SPAG5	28578086	T	G	0.348	ENSP00000323300.5:p.Asn1145Thr	rs138772502	0.0014
chr17	KRTAP29-1	41302224	A	T	0.678	ENSP00000375148.1:p.Cys210Ser		
chr17	KRT33B	41364890	C	T	0.486	ENSP00000251646.3:p.Arg329His		
chr17	KRT33B	41369498	C	T	0.567	ENSP00000251646.3:p.Glu85Lys		
chr17	ETV4	43528697	G	A	0.278	ENSP00000321835.4:p.Ala426Val	rs117364926	0.001
chr17	KANSL1	46171833	T	G	0.215	ENSP00000387393.3:p.Lys104Thr		
chr17	EPN3	50536971	C	T	0.676	ENSP00000268933.3:p.Arg139Trp	rs371737517	0.0002
chr17	ACE	63491216	C	T	0.234	ENSP00000290866.4:p.Thr916Met	rs3730043	0.0034
chr17	CSH2	63872181	T	C	0.178	ENSP00000376623.2:p.Glu200Gly		
chr18	PIEZO2	10671669	C	T	0.134	ENSP00000421377.3:p.Arg2706Gln	rs189453524	0.0004
chr18	OSBPL1A	24167436	A	G	0.265	ENSP00000320291.3:p.Ser810Pro	rs35693789	0.0094
chr19	PODNL1	13934406	C	T	0.234	ENSP00000345175.4:p.Val174Met	rs781238470	
chr19	PALM3	14053817	C	T	0.376	ENSP00000344996.3:p.Asp604Asn	rs75841596,COSM1390897	0.0116
chr19	WTIP	34482629	C	T	0.184	ENSP00000466953.2:p.Arg219Trp		
chr19	ZNF599	34769537	C	T	0.180	ENSP00000333802.6:p.Asp13Asn	rs117610843	0.0058
chr19	CYP2A6	40848628	A	T	0.256	ENSP00000301141.4:p.Leu160His	rs1801272,CM980517	0.0092
chr19	PPP1R37	45144962	C	T	0.324	ENSP00000221462.3:p.Leu366Phe	rs146723120	0.003
chr19	NOP53	47745650	G	C	0.134	ENSP00000246802.4:p.Asp31His	rs78530808	0.0158
chr19	NTN5	48664274	A	G	0.102	ENSP00000270235.3:p.Ile280Thr	rs142533877	0.0056

chr19	LILRB2	54279040	G	A	0.304	ENSP00000375629.4:p.Leu243Phe	COSM1326184	
chr19	LILRA2	54574799	C	A	0.356	ENSP00000251377.3:p.Leu141Ile		
chr19	LILRA2	54575019	A	G	0.405	ENSP00000251377.3:p.Glu214Gly		
chr19	KIR2DL1	54773491	C	A	0.546	ENSP00000336769.5:p.His77Asn		
chr19	KIR2DL1	54773534	C	A	0.625	ENSP00000336769.5:p.Thr91Lys	COSM5712917,COSM5545196,COSM3404605	
chr19	KIR2DL4	54804874	A	G	0.645	ENSP00000339634.5:p.Tyr53Cys		
chr19	KIR3DL1	54819832	G	T	0.654	ENSP00000375608.4:p.Gly159Trp		
chr19	KIR3DL2	54865893	G	C	0.564	ENSP00000325525.3:p.Trp363Cys		
chr20	PYGB	25276685	T	C	0.678	ENSP00000216962.3:p.Tyr234His		
chr20	ANKRD60	58218668	G	A	0.564	ENSP00000396747.1:p.Pro289Ser	rs41275658	0.002
chr20	LAMA5	62317394	C	T	0.304	ENSP00000252999.3:p.Ala2488Thr	rs148169370	0.0048
chr22	IGLV5-45	22376251	C	T	0.234	ENSP00000374831.2:p.Leu39Phe		
chr22	GSTTP1	23998546	C	A	0.215	ENSP00000492273.1:p.Arg241Met		
chr22	GSTTP1	23998547	T	A	0.435	ENSP00000492273.1:p.Arg241Trp		
chr22	SUSD2	24183189	G	T	0.180	ENSP00000351075.3:p.Gly70Val	rs79232038	
chr22	KIAA1671	25029315	A	G	0.376	ENSP00000351207.3:p.Lys439Arg		
chr22	CYP2D6	42127526	C	T	0.128	ENSP00000353820.5:p.Arg365His	rs1058172	
chr22	CYP2D6	42130692	G	A	0.166	ENSP00000353820.5:p.Pro34Ser	CM900081	
chr22	TUBGCP6	50221169	C	T	0.924	ENSP00000248846.5:p.Gly1064Arg	rs149231425	0.0132
chr22	PLXNB2	50280899	A	G	0.184	ENSP00000409171.1:p.Tyr1280His	COSM4444878	
chrX	PAGE1	49689423	T	C	1.000	ENSP00000365320.3:p.Glu138Gly	rs151117508	0.0079
					0.567		rs111638770,COSM5461083,COSM5461082,COSM388435	
chrX	FAM104B	55146247	G	C		ENSP00000397188.2:p.Pro63Arg		
chrX	MED12	71119383	C	G	0.215	ENSP00000363193.3:p.Thr37Arg		
chrX	RTL9	110450737	G	C	1.000	ENSP00000419786.2:p.Gln40His	rs150383653,COSM4721270	0.0003
chrX	SLC25A5	119469766	G	A	0.345	ENSP00000360671.4:p.Gly73Ser	rs143413528	
chrX	SLC25A5	119469779	A	C	0.204	ENSP00000360671.4:p.Asn77Thr	rs148294496	
chrX	SLC25A5	119469784	A	T	0.184	ENSP00000360671.4:p.Ile79Phe	rs141428607	

chrX SLC25A5 119470481 G C 0.444 ENSP00000360671.4:p.Arg236Pro rs114413582

Table S3. Mutations found in the WES for chromosome/telomere instability and the VEGF-angiogenesis pathway in sporadic CAS sequenced individuals (non-*POT1* mutation carriers).

Pathway	Sample	Gene	Genomic position	Reference allele	Alternative allele	ALT Allelic fraction	Amino acid change	dbsnp	MAF
Mutations involved in damage response and repair	NT1*	<i>TP53BP2</i>	223991119	G	T	0.213	Q229K	rs34683843	0.0467
	NT2*	<i>TP53BP1</i>	43762077	TGGGATAGG	TGG	0.205	PI454-		
	NT3*	<i>ATR</i>	142215368	GGAAGTAA	-	0.215			
		<i>ATM</i>	108200982	T	A	0.166	L2450*		
		<i>BRCA2</i>	32912956	C	A	0.166	H1488Q		
	T1	<i>BRCA1</i>	41245120	T	A	0.128	N810Y	rs28897682	
		<i>BRCA1</i>	41246481	T	C	0.257	Q356R	rs1799950	0.0279
		<i>TP53</i>	7578503	C	T	0.451	V143M		
		<i>TP53RK</i>	45315786	C	T	0.255	R123Q	rs34983477	0.0279
		<i>APC2</i>	1457002	G	C	0.376	G323R	rs143870588	0.0119
	T2	<i>TP53BP2</i>	223998162	G	A	0.201	P115S		
	T3	<i>BRCA1</i>	41245471	C	T	0.312	D693N	rs4986850	0.0398
		<i>RAD51C</i>	56798128	A	G	0.255	T287A	rs28363317	0.0055
		<i>ATM</i>	108165638	TTTAGGAAAT TAACCATTTT CTCT	-	0.423	-1593		
		<i>CDK8</i>	26911760	C	T	0.310	S62L		
		<i>BRIP1</i>	59861662	C	A	0.567	V533L		
	T4	<i>TP53</i>	7576876	C	G	0.346	D324H		
		<i>TP53</i>	7578406	C	T	0.134	R175H	rs28934578	
		<i>RAD51B</i>	68331765	A	T	0.126	M121L	rs150928231	
		<i>RAD51B</i>	68352648	T	G	0.104	L172W	rs34094401	0.0188
	<i>ATM</i>	108123551	C	T	0.104	P604S	rs2227922	0.0032	
	<i>APC2</i>	1468408	C	A	0.376	A1703E	rs200444154		
NT2*; T3	<i>ATM</i>	108175462	G	A	0-202	D1853N	rs1801516	0.0788	

Mutations involved in Angiogenesis	NT1**	<i>KDR</i>	55979558	C	T	0.184	V297I	rs2305948	0.1310
		<i>RASA2</i>	141326602	T	C	0.422		rs295322	0.1140
		<i>DOCK1</i>	128810642	C	T	0.273		rs9418773	0.1230
		<i>RICTOR</i>	38952300	G	A	0.179	S1042L		
		<i>IQGAP1</i>	90996087	G	A	0.189	E415K	rs200988874	0.0005
		<i>SRC</i>	36012590	A	G	0.304	S12G		
		<i>PIK3C2G</i>	18691253	C	T	0.435		rs12315010	0.0389
	NT2*	<i>NRAS</i>	115256530	G	T	0.134	Q61K	rs121913254	
		<i>PDPK1</i>	2607915	CT	C	0.310	-79		
		<i>RASA4</i>	102246366	G	A	0.124	R123W	rs139960113	0.0020
	NT3*	<i>SHOX2</i>	157823580	TACA	T	0.556	p.77_78del		
		T1	<i>NRG2</i>	139231255	C	T	0.345	R577H	rs75431091
	<i>SPTAN1</i>		131367372	A	G	0.204	N1260S		
	<i>FGF22</i>		640065	C	T	0.256	S47F		
	T2	<i>PIK3C2G</i>	18443809	C	A	0.107	A261E	rs7133666	0.0417
		<i>RASA2</i>	141299289	G	A	0.172	S557N		
		<i>MAP2K1</i>	66736993	G	T	0.243			
		<i>IQGAP1</i>	91025227	T	G	0.435	L1122R		
		<i>VAV3</i>	108145045	C	T	0.172	E732K		
		<i>DUSP8</i>	1579018	T	C	0.234		rs113161544	0.0640
		<i>PIK3C2G</i>	18473929	C	T	0.432	Q391*		
	T3	<i>RASA2</i>	141328901	G	A	0.134	G839R		
		<i>PLCG1</i>	39792063	A	G	0.345	S279G	rs2228246	0.0952
		<i>RICTOR</i>	38960053	C	T	0.180	V627I		
		<i>DUSP8</i>	1579506	A	G	0.172			
		<i>RASA4</i>	102235804	G	A	0.102	T340I		
		<i>RASA4</i>	102246393	C	T	0.165	E114K		
	T4	<i>ITGAV</i>	187540655	G	A	0.184			
		<i>PTPRQ</i>	81004265	A	C	0.436	E1589D		
<i>PIK3C2G</i>		18656259	C	T	0.174	H1021Y	rs201569993	0.0006	

	<i>PRKCQ</i>	6498721	G	A	0.102	A521V	
T1; T3; T4	<i>SPTANI</i>	131377915	G	A	0.304	R1718H	
T3; NT1*	<i>MAP2K1</i>	66777404	C	T	0.174	A257V	
T4; NT2*	<i>VEGFA</i>	43738526	C	G	0.184	A28G	rs201786558

* Confirmed constitutional ** Confirmed somatic.

Table S4. Actionable variants found in the sequencing experiment with IBM Watson for Genomics platform for T1 patient.

Gene	Actionable variant	Variant evidence (Pubmed)	FDA-approved drug for Angiosarcoma	Other molecules with clinical evidence (NCT)
<i>MSH6</i>	p.Glu1088fs	12019211	Pembrolizunab	Nivolumab (NCT0366819)
<i>TP53</i>	p.Arg175His	8510927; 17401432	-	Adavosertib (NCT01827384) Transferrin (NCT02354547)
<i>ARID1A</i>	p.Pro21del	23097632	-	**
<i>ATR</i>	p.Ile774fs	22960745	-	**
<i>NOTCH</i>	p.Pro2415del	15472975*; 25564152*	-	**

NCT: Number of Clinical Trial

* Similar variant within the same domain.

** Compelling preclinical evidence and/or case study reports support the biomarker as being predictive of response to this drug

Table S5. Actionable variants found in the sequencing experiment with IBM Watson for Genomics platform for T4 patient.

Gene	Actionable variant	Variant evidence (Pubmed)	FDA-approved drug for Angiosarcoma	Other molecules with clinical evidence (NCT)
<i>CDK2A</i>	p.Arg99Pro	20340136; 19260062	-	Palbociclib (NCT03239015)
<i>TP53</i>	p.Val143Met	23469205	-	Adavosertib (NCT01827384) Transferrin (NCT02354547)
<i>KIT</i>	Amplification	21523721; 17189383; 16166280	Pazopanib (NCT01462630)*	Pazopanib (NCT03628131) Imatinib (NCT02461849) Nilotinib (NC02379416)

NCT: Number of Clinical Trial

* Phase II study